WEST

Freeform Search

Database:
US Patents Full-Text Database
US Pre-Grant Publication Full-Text Database
JPO Abstracts Database
EPO Abstracts Database
Derwent World Patents Index
IBM Technical Disclosure Bulletins

Term: (defficien$ or delet$ or knockout or null) near8 (elastin or tropoelastin)

Display: 20 **Documents in Display Format:** - **Starting with Number** 1

Generate: ○ Hit List ◉ Hit Count ○ Side by Side ○ Image

Search | Clear | Help | Logout | Interrupt

Main Menu | Show S Numbers | Edit S Numbers | Preferences | Cases

Search History

DATE: Wednesday, January 15, 2003 Printable Copy Create Case

Set Name side by side	**Query**	**Hit Count**	**Set Name** result set
	DB=USPT,PGPB; PLUR=YES; OP=AND		
L5	L1 and ((800/14)!.CCLS.)	0	L5
L4	L1 and ((800/13)!.CCLS.)	0	L4
L3	l1 and ((800/8)!.CCLS.)	0	L3
L2	l1 with (mouse or animal or mice or sheep or rabbit or bovine or cow or pig)	0	L2
L1	(defficien$ or delet$ or knockout or null) near8 (elastin or tropoelastin)	11	L1

END OF SEARCH HISTORY

Generate Collection | Print

Search Results - Record(s) 1 through 11 of 11 returned.

☐ 1. 20020103353 . 09 Mar 01. 01 Aug 02. Sequences characteristic of hypoxia-regulated gene transcription. Einat, Paz, et al. 536/23.2; 435/320.1 435/325 435/69.1 C07H021/04 C12P021/02 C12N005/06.

☐ 2. 20010007756 . 09 Mar 98. 12 Jul 01. COSMETIC COMPOSITIONS. ENSLEY, BURT D.. 435/69.1; 435/320.1 514/773 524/401 530/323 C12P021/06 C12N015/09 C12N015/74 A01N025/00 C12N015/00 C08J003/00 A61K047/00.

☐ 3. 6451326 . 09 Mar 98; 17 Sep 02. Cosmetic compositions. Ensley; Burt D.. 424/401; 424/59 424/69 424/78.03 435/69.1 514/12 514/2 530/350. A61K006/00 A61K007/42 A61K007/035 A61K031/74 C12P021/06.

☐ 4. 6365623 . 30 Dec 99; 02 Apr 02. Treatment of acne using lipoic acid. Perricone; Nicholas V.. 514/448; 514/458 514/724 514/725. A61K031/38 A61K031/355 A61K031/045 A61K031/07.

☐ 5. 6277622 . 08 Feb 99; 21 Aug 01. Synthetic polynucleotides. Weiss; Anthony Steven. 435/252.3; 435/183 435/189 435/41 435/440 435/69.1 536/23.1 536/23.2. C12N001/20 C12N009/02 C07H021/04.

☐ 6. 6232458 . 24 Jul 95; 15 May 01. Synthetic polynucleotides encoding tropoelastin. Weiss; Anthony Steven, et al. 536/23.5; 435/252.33 435/254.1 435/254.2 435/320.1 435/69.1 435/69.7 530/353 536/23.4 536/24.1 536/24.2. C07H021/04 A61K038/39 C12N001/21.

☐ 7. 6018098 . 23 Dec 97; 25 Jan 00. In vivo and in vitro model of cutaneous photoaging. Bernstein; Eric F., et al. 623/16.11; 424/9.1 424/9.2 435/325 435/352 435/357 800/3. C12N015/00 C12N015/85 A61K049/00 C12Q001/00.

☐ 8. 5858662 . 10 Jul 96; 12 Jan 99. Diagnosis of Williams syndrome and Williams syndrome cognitive profile by analysis of the presence or absence of a LIM-kinase gene. Keating; Mark T., et al. 435/6; 435/91.1 435/91.2 536/23.1 536/23.5 536/24.31 536/24.33. C12Q001/68 C12P019/34 C12N015/00.

☐ 9. 5840489 . 07 Jun 95; 24 Nov 98. Diagnosis and treatment of supravalvular aortic stenosis and Williams syndrome. Keating; Mark T., et al. 435/6; 435/91.1 435/91.2 536/23.1 536/23.5 536/24.31 536/24.33. C12Q001/68 C12P019/34 C07H021/02 C12N015/00.

☐ 10. 5726040 . 02 May 96; 10 Mar 98. Cosmetic compositions including tropoelastin isomorphs. Ensley; Burt D., et al. 435/69.1; 424/401 424/59 424/69 424/78.03 435/252.3 435/252.33 435/320.1 435/325 435/366 435/69.7 435/69.8 514/12 514/2 530/350 530/353. C12P021/06 A61K007/035 A61K007/42 A61K038/16.

☐ 11. 5650282 . 07 Jun 95; 22 Jul 97. Diagnosis of Williams syndrome. Keating; Mark T., et al. 435/6; 435/270 435/91.1 435/968 436/94 536/23.1 536/23.5 536/24.31 536/24.33. C12Q001/68 C12P019/34 C07H021/04 C12N015/00.

Generate Collection Print

Terms	Documents
(defficien$ or delet$ or knockout or null) near8 (elastin or tropoelastin)	11

Previous Page Next Page

```
=> d his

     (FILE 'HOME' ENTERED AT 17:35:41 ON 15 JAN 2003)

     FILE 'MEDLINE, CAPLUS, BIOSIS, SCISEARCH' ENTERED AT 17:36:02 ON 15 JAN
     2003
L1          613 S (DEFICIEN? OR DELET? OR KNOCKOUT OR NULL)(8A)(ELASTIN OR TROP
L2     12321616 S MOUSE OR MICE OR ANIMAL OR SHEEP OR BOVINE OR COW OR PIG OR R
L3          155 S L1(S)L2
L4           85 DUP REM L3 (70 DUPLICATES REMOVED)

=> d au ti so 30-85 l4

L4   ANSWER 30 OF 85     MEDLINE                            DUPLICATE 15
AU   Starcher B; Conrad M
TI   A role for neutrophil elastase in solar elastosis.
SO   CIBA FOUNDATION SYMPOSIUM, (1995) 192 338-46; discussion 346-7.  Ref: 6
     Journal code: 0356636. ISSN: 0300-5208.

L4   ANSWER 31 OF 85  CAPLUS  COPYRIGHT 2003 ACS
AU   Dallapiccola, B.; Amati, F.; Gennarelli, M.; Mari, A.; Novelli, G.
TI   Advances in molecular analysis of congenital heart defects
SO   Bulletin of Molecular Biology and Medicine (1995), 20(3,4), 135-140
     CODEN: BMBMD5; ISSN: 0391-481X

L4   ANSWER 32 OF 85  SCISEARCH  COPYRIGHT 2003 ISI (R)
AU   STARCHER B (Reprint); CONRAD M
TI   A ROLE FOR NEUTROPHIL ELASTASE IN THE PROGRESSION OF SOLAR ELASTOSIS
SO   CONNECTIVE TISSUE RESEARCH, (1995) Vol. 31, No. 2, pp. 133-140.
     ISSN: 0300-8207.

L4   ANSWER 33 OF 85  CAPLUS  COPYRIGHT 2003 ACS
AU   Lowery, Mary C.; Morris, Colleen A.; Ewart, Amanda; Brothman, Lisa J.;
     Zhu, Xiao Lin; Leonard, Claire O.; Carey, John C.; Keating, Mark;
     Brothman, Arthur R.
TI   Strong correlation of elastin deletions, detected by FISH, with Williams
     syndrome: evaluation of 235 patients
SO   American Journal of Human Genetics (1995), 57(1), 49-53
     CODEN: AJHGAG; ISSN: 0002-9297

L4   ANSWER 34 OF 85  CAPLUS  COPYRIGHT 2003 ACS
AU   Ewart, Amanda K.; Jin, Weishan; Atkinson, Donald; Morris, Colleen A.;
     Keating, Mark T.
TI   Supravalvular aortic stenosis associated with a deletion disrupting the
     elastin gene
SO   Journal of Clinical Investigation (1994), 93(3), 1071-7
     CODEN: JCINAO; ISSN: 0021-9738

L4   ANSWER 35 OF 85     MEDLINE                            DUPLICATE 16
AU   Grosso L E; Scott M
TI   PGAIPG, a repeated hexapeptide of bovine and human tropoelastin, is
     chemotactic for neutrophils and Lewis lung carcinoma cells.
SO   ARCHIVES OF BIOCHEMISTRY AND BIOPHYSICS, (1993 Sep) 305 (2) 401-4.
     Journal code: 0372430. ISSN: 0003-9861.

L4   ANSWER 36 OF 85     MEDLINE                            DUPLICATE 17
AU   Blankenship J W; McKinney B C; Roos P J; Sandberg L B
TI   Quantitation of lung elastin and collagen in protein and essential fatty
     acid malnourished rats.
SO   CONNECTIVE TISSUE RESEARCH, (1993) 29 (4) 311-8.
     Journal code: 0365263. ISSN: 0300-8207.

L4   ANSWER 37 OF 85     MEDLINE
AU   Latge J P; Debeaupuis J P; Sarfati J; Diaquin M; Paris S
```

TI Cell wall antigens in Aspergillus fumigatus.
SO ARCHIVES OF MEDICAL RESEARCH, (1993 Autumn) 24 (3) 269-74. Ref: 36
Journal code: 9312706. ISSN: 0188-4409.

L4 ANSWER 38 OF 85 CAPLUS COPYRIGHT 2003 ACS
AU Martorana, Piero A.; Brand, Thomas; Gardi, Concetta; Van Even, Paul; De Santi, M. Margherita; Calzoni, Paola; Marcolongo, Paola; Lungarella, Giuseppe
TI The pallid mouse: a model of genetic .alpha.1-antitrypsin deficiency
SO Laboratory Investigation (1993), 68(2), 233-41
CODEN: LAINAW; ISSN: 0023-6837

L4 ANSWER 39 OF 85 MEDLINE DUPLICATE 18
AU Grosso L E; Scott M
TI PGAIPG, a repeated hexapeptide of bovine tropoelastin, is a ligand for the 67-kDa bovine elastin receptor.
SO MATRIX, (1993 Mar) 13 (2) 157-64.
Journal code: 8906139. ISSN: 0934-8832.

L4 ANSWER 40 OF 85 CAPLUS COPYRIGHT 2003 ACS
AU Ewart, Amanda K.; Morris, Colleen A.; Atkinson, Donald; Jin, Weishan; Sternes, Keith; Spallone, Patricia; Stock, A. Dean; Leppert, Mark; Keating, Mark T.
TI Hemizygosity at the elastin locus in a developmental disorder, Williams syndrome
SO Nature Genetics (1993), 5(1), 11-16
CODEN: NGENEC; ISSN: 1061-4036

L4 ANSWER 41 OF 85 MEDLINE DUPLICATE 19
AU Hinek A; Boyle J; Rabinovitch M
TI Vascular smooth muscle cell detachment from elastin and migration through elastic laminae is promoted by chondroitin sulfate-induced "shedding" of the 67-kDa cell surface elastin binding protein.
SO EXPERIMENTAL CELL RESEARCH, (1992 Dec) 203 (2) 344-53.
Journal code: 0373226. ISSN: 0014-4827.

L4 ANSWER 42 OF 85 MEDLINE DUPLICATE 20
AU Parks W C; Roby J D; Wu L C; Grosso L E
TI Cellular expression of tropoelastin mRNA splice variants.
SO MATRIX, (1992 Apr) 12 (2) 156-62.
Journal code: 8906139. ISSN: 0934-8832.

L4 ANSWER 43 OF 85 CAPLUS COPYRIGHT 2003 ACS
AU Boyd, Charles D.; Christiano, Angela M.; Pierce, Richard A.; Stolle, Catherine A.; Deak, Susan B.
TI Mammalian tropoelastin: multiple domains of the protein define an evolutionarily divergent amino acid sequence
SO Matrix (Stuttgart) (1991), 11(4), 235-41
CODEN: MTRXEH; ISSN: 0934-8832

L4 ANSWER 44 OF 85 MEDLINE DUPLICATE 21
AU Pierce R A; Deak S B; Stolle C A; Boyd C D
TI Heterogeneity of rat tropoelastin mRNA revealed by cDNA cloning.
SO BIOCHEMISTRY, (1990 Oct 16) 29 (41) 9677-83.
Journal code: 0370623. ISSN: 0006-2960.

L4 ANSWER 45 OF 85 MEDLINE DUPLICATE 22
AU Starcher B; Williams I
TI The beige mouse: role of neutrophil elastase in the development of pulmonary emphysema.
SO EXPERIMENTAL LUNG RESEARCH, (1989 Sep) 15 (5) 785-800.
Journal code: 8004944. ISSN: 0190-2148.

```
=> d 31 40 au ti so ab l4

L4   ANSWER 31 OF 85  CAPLUS  COPYRIGHT 2003 ACS
AU   Dallapiccola, B.; Amati, F.; Gennarelli, M.; Mari, A.; Novelli, G.
TI   Advances in molecular analysis of congenital heart defects
SO   Bulletin of Molecular Biology and Medicine (1995), 20(3,4), 135-140
     CODEN: BMBMD5; ISSN: 0391-481X
AB   Linkage anal. and mol. studies directed by chromosome abnormalities have
     been used to search for genes related to congenital heart defects.
     Exclusion mapping of a gene for autosomal dominant atrioventricular canal
     defect from the crit. distal 21p and 8p regions has been obtained by
     linkage studies in two pedigrees.  A search for deletions at 22q11 in 201
     patients with conotruncal defects has showed hemizygosity only in those
     with dysmorphisms or malformations typical of DiGeorge and
     velo-cardio-facial syndromes.  Haploinsufficiency at 22q11 was found also
     in patients with transposition of great arteries, either with an intact
     septum or ventricular septal defects.  Deletion of the elastin gene was
     found in a series of 54 patients with Williams syndrome, supporting that
     elastin hemizygosity is pathogenetically related to this disorder.

L4   ANSWER 40 OF 85  CAPLUS  COPYRIGHT 2003 ACS
AU   Ewart, Amanda K.; Morris, Colleen A.; Atkinson, Donald; Jin, Weishan;
     Sternes, Keith; Spallone, Patricia; Stock, A. Dean; Leppert, Mark;
     Keating, Mark T.
TI   Hemizygosity at the elastin locus in a developmental disorder, Williams
     syndrome
SO   Nature Genetics (1993), 5(1), 11-16
     CODEN: NGENEC; ISSN: 1061-4036
AB   Williams syndrome (WS) is a developmental disorder affecting connective
     tissue and the central nervous system.  A common feature of WS,
     supravalvular aortic stenosis, is also a distinct autosomal dominant
     disorder caused by mutations in the elastin gene.  In this study the
     authors identified hemizygosity at the elastin locus using genetic
     analyses in four familial and five sporadic cases of WS.  Fluorescent in
     situ hybridization and quant. Southern analyses confirmed these findings,
     demonstrating inherited and de novo deletions of the elastin gene.  These
     data indicate that deletions involving one elastin allele cause WS and
     implicate elastin hemizygosity in the pathogenesis of the disease.


=> d au ti so 1-29 ab l4

L4   ANSWER 1 OF 85  CAPLUS  COPYRIGHT 2003 ACS
AU   Nakamoto, Tetsuya; Suzuki, Takahiro; Huang, Jinhong; Matsumura, Tomoko;
     Seo, Sachiko; Honda, Hiroaki; Sakai, Ryuichi; Hirai, Hisamaru
TI   Analysis of gene expression profile in p130Cas-deficient fibroblasts
SO   Biochemical and Biophysical Research Communications (2002), 294(3),
     635-641
     CODEN: BBRCA9; ISSN: 0006-291X
AB   P130Cas (Cas) is a docking protein that becomes tyrosine phosphorylated in
     v-Src- or v-Crk-transformed cells and in integrin-stimulated cells.  Cas
     -/- fibroblasts show defects in stress fiber formation, cell spreading,
     cell migration, and transformation by activated Src.  To further
     characterize the role of Cas in signaling, we compared the expression
     profile in Cas -/- fibroblasts with that in Cas-re-expressing fibroblasts
     using the microarray methods.  In Cas -/- fibroblasts, the expression of
     heme oxygenase 1 and caveolin-1 was reduced, but the expression of
     procollagen 1 .alpha. 1, procollagen 3 .alpha. 1, procollagen 11 .alpha.
     1, elastin, periostin, TSC-36, and MARCKS was enhanced.  The domains in
     Cas necessary for the change varied among these genes.  Activated Src
     reduced the expression of most of these genes both in Cas -/- and in Cas
     +/+ fibroblasts.  These results suggest the existence of signaling
     pathways that emanate from Cas to gene expression.
```

L4 ANSWER 2 OF 85 MEDLINE DUPLICATE 1
AU Vouyouka A G; Pfeiffer B J; Liem T K; Taylor T A; Mudaliar J; Phillips C L
TI The role of type I collagen in aortic wall strength with a homotrimeric.
SO JOURNAL OF VASCULAR SURGERY, (2001 Jun) 33 (6) 1263-70.
Journal code: 8407742. ISSN: 0741-5214.
AB PURPOSE: Elastin and collagen (types I and III) are the primary load-bearing elements in aortic tissue. **Deficiencies** and derangements in **elastin** and type III collagen have been associated with the development of aneurysmal disease. However, the role of type I collagen is less well defined. The purpose of this study was to define the role of type I collagen in maintaining biomechanical integrity in the thoracic aorta, with a **mouse** model that produces homotrimeric type I collagen [alpha1(I)]3, rather than the normally present heterotrimeric [alpha1(I)]2 alpha2(I) type I collagen isotype. METHODS: Ascending and descending thoracic aortas from homozygous (oim/oim), heterozygous (oim /+), and wildtype (+/+) **mice** were harvested. Circumferential and longitudinal load-extension curves were used as a means of determining maximum breaking strength (Fmax) and incremental elastic modulus (IEM). Histologic analyses and hydroxyproline assays were performed as a means of determining collagen organization and content. RESULTS: Circumferentially, the ascending and descending aortas of oim /oim **mice** demonstrated significantly reduced Fmax, with an Fmax of only 60% and 23%, respectively, of wildtype **mice** aortas. Oim/oim descending aortas demonstrated significantly greater compliance (decreased IEM), and the ascending aortas also exhibited a trend toward increased compliance. Reduced breaking strength was also demonstrated with longitudinal extension of the descending aorta. CONCLUSION: The presence of homotrimeric type I collagen isotype (absence of alpha2(I) collagen) significantly weakens the aorta. This study demonstrates the integral role of type I collagen in the biomechanical and functional properties of the aorta and may help to elucidate the role of collagen in the development of aneurysmal aortic disease or dissection.

L4 ANSWER 3 OF 85 MEDLINE DUPLICATE 2
AU Kumashiro K K; Kim M S; Kaczmarek S E; Sandberg L B; Boyd C D
TI (13)C cross-polarization/magic angle spinning NMR studies of alpha-elastin preparations show retention of overall structure and reduction of mobility with a decreased number of cross-links.
SO BIOPOLYMERS, (2001 Oct 5) 59 (4) 266-75.
Journal code: 0372525. ISSN: 0006-3525.
AB High-resolution solid-state (13)C NMR spectra are presented for samples of alpha-**elastin** prepared from the aorta of normal and copper-**deficient pigs**. Chemical shifts of the various peaks indicate that both the normal and undercross-linked peptides have similar overall structures. However, (13)C T(1), (13)C T(1 rho), and (1)H T(1 rho) measurements indicate that the alpha-elastin peptides obtained from the abnormal elastic fibers samples exhibit altered mobilities, particularly in their side chains. Results from spectra taken with a range of contact times and from dipolar dephasing experiments are consistent with conclusions reached with the relaxation measurements. Namely, the loss of function associated with the undercross-linked sample is correlated to a small but measurable difference in relative mobility.
Copyright 2001 John Wiley & Sons, Inc. Biopolymers 59: 266-275, 2001

L4 ANSWER 4 OF 85 MEDLINE DUPLICATE 3
AU Faury G
TI [Role of elastin in the development of vascular function. Knock-out study of the elastin gene in mice].
Role de l'elastine dans le developpement et la fonction vasculaires. Etude par knock-out du gene de l'elastine chez la souris.
SO JOURNAL DE LA SOCIETE DE BIOLOGIE, (2001) 195 (2) 151-6. Ref: 34
Journal code: 100890617.
AB The elastic fibres endow extensible tissues with resiliency, such as in

blood vessels, heart, skin and lung. Elastic fibres are made of microfibrils, and mainly elastin (90%) which provides the fibre with elasticity. Beside the biomechanical role of elastin, a close correlation between elastin and elastic fibre network disorganisation and vascular smooth muscle cell (VSMC) growth disregulation has been known for several years through the description and study of several human or **animal** polyfeatured or obstructive vascular diseases, such as supravalvular aortic stenosis (SVAS) and Williams syndrome (WS), both related to heterozygous mutations or **deletion** in the **elastin** gene. The study of **mice** knock-out for the elastin gene (homozygous or heterozygous) leads to think that elastin should now be seen as an important elastic component providing extensible tissues with resiliency, as well as a major developmental regulator of VSMC life cycle and smooth muscle tissue organisation. Further developments in the area of preventive therapy of SVAS, WS or other inherited muscular disorders are likely to arise from these results.

L4 ANSWER 5 OF 85 CAPLUS COPYRIGHT 2003 ACS
AU Hinek, Aleksander; Smith, Adam C.; Cutiongco, Eva Maria; Callahan, John W.; Gripp, Karen W.; Weksberg, Rosanna
TI Decreased elastin deposition and high proliferation of fibroblasts from Costello syndrome are related to functional deficiency in the 67-kD elastin-binding protein
SO American Journal of Human Genetics (2000), 66(3), 859-872
CODEN: AJHGAG; ISSN: 0002-9297
AB Costello syndrome is characterized by mental retardation, loose skin, coarse face, skeletal deformations, cardiomyopathy, and predisposition to numerous malignancies. The genetic origin of Costello syndrome has not yet been defined. Using immunohistochem. and metabolic labeling with [3H]-valine, we have established that cultured skin fibroblasts obtained from patients with Costello syndrome did not assemble elastic fibers, despite an adequate synthesis of tropoelastin and normal deposition of the microfibrillar scaffold. We found that impaired prodn. of elastic fibers by these fibroblasts is assocd. with a functional deficiency of the 67-kD elastin-binding protein (EBP), which is normally required to chaperone tropoelastin through the secretory pathways and to its extracellular assembly. Metabolic pulse labeling of the 67-kD EBP with radioactive serine and further chase of this tracer indicated that both normal fibroblasts and fibroblasts from patients with Costello syndrome initially synthesized comparable amts. of this protein; however, the fibroblasts from Costello syndrome patients quickly lost it into the conditioned media. Because the normal assocn. between EBP and tropoelastin can be disrupted on contact with galactosugar-bearing moieties, and the fibroblasts from patients with Costello syndrome revealed an unusual accumulation of chondroitin sulfate-bearing proteoglycans (CD44 and biglycan), we postulate that a chondroitin sulfate may be responsible for shedding EBP from Costello cells and in turn for their impaired elastogenesis. This was further supported by the fact that exposure to chondroitinase ABC, an enzyme capable of chondroitin sulfate degrdn., restored normal prodn. of elastic fibers by fibroblasts from patients with Costello syndrome. We also present evidence that loss of EBP from fibroblasts of Costello syndrome patients is assocd. with an unusually high rate of cellular proliferation.

L4 ANSWER 6 OF 85 MEDLINE DUPLICATE 4
AU Betsuyaku T; Fukuda Y; Parks W C; Shipley J M; Senior R M
TI Gelatinase B is required for alveolar bronchiolization after intratracheal bleomycin.
SO AMERICAN JOURNAL OF PATHOLOGY, (2000 Aug) 157 (2) 525-35.
Journal code: 0370502. ISSN: 0002-9440.
AB Increased expression of matrix metalloproteinases, particularly gelatinase B (MMP-9), has been described in the lungs in pulmonary fibrosis. Intratracheal bleomycin is often used experimentally to produce lesions resembling human fibrosing alveolitis. To assess the role of gelatinase B

in bleomycin-induced fibrosing alveolitis, we instilled bleomycin intratracheally into gelatinase B-deficient **mice** and gelatinase B+/+ littermates. Twenty-one days after bleomycin the two groups of **mice** were indistinguishable in terms of pulmonary histology and total lung collagen and **elastin**. However, the lungs of gelatinase B-**deficient mice** showed minimal alveolar bronchiolization, whereas bronchiolization was prominent in the lungs of gelatinase B+/+ **mice**. Gelatinase B was identified immunohistochemically in terminal bronchiolar cells and bronchiolized cells 7 and 14 days after bleomycin in gelatinase B+/+ **mice**, and whole lung gelatinase B mRNA was increased at the same times. Many bronchiolized cells displayed Clara cell features by electron microscopy. Some bronchiolized cells stained with antibody to helix transcription factor 4, a factor associated with the ciliated cell phenotype. Thus, fibrosing alveolitis develops after intratracheal bleomycin irrespective of gelatinase B. However, gelatinase B is required for alveolar bronchiolization, perhaps by facilitating migration of Clara cells and other bronchiolar cells into the regions of alveolar injury.

L4 ANSWER 7 OF 85 MEDLINE DUPLICATE 5
AU Klevay L M
TI Cardiovascular disease from copper deficiency--a history.
SO JOURNAL OF NUTRITION, (2000 Feb) 130 (2S Suppl) 489S-492S.
Journal code: 0404243. ISSN: 0022-3166.
AB Although the nutritional essentiality of copper was established in 1928, a preoccupation with hematology delayed the discovery of cardiovascular disease from copper deficiency for more than a decade. Anatomical studies of several species of deficient **animals** revealed, interalia, aortic fissures and rupture, arterial foam cells and smooth muscle migration, cardiac enlargement and rupture, coronary artery thrombosis and myocardial infarction. Abnormal biochemistry in deficiency probably contributes to these lesions, e.g., decreased activities of lysyl oxidase and superoxide dismutase which result in failure of collagen and **elastin** crosslinking and impaired defense against free radicals. Copper **deficiency** also decreases copper in hearts and other organs and cells and increases cholesterol in plasma. Abnormal physiology from deficiency includes abnormal electrocardiograms, glucose intolerance and hypertension. People with ischemic heart disease have decreased cardiac and leucocyte copper and decreased activities of some copper-dependent enzymes. Copper depletion experiments with men and women have revealed abnormalities of lipid metabolism, blood pressure control, and electrocardiograms plus impaired glucose tolerance. The Western diet often is as low in copper as that proved insufficient for these people. Knowledge of nutritional history can be useful in addressing contemporary nutritional problems.

L4 ANSWER 8 OF 85 MEDLINE DUPLICATE 6
AU Dietz H C; Mecham R P
TI Mouse models of genetic diseases resulting from mutations in elastic fiber proteins.
SO MATRIX BIOLOGY, (2000 Nov) 19 (6) 481-8. Ref: 42
Journal code: 9432592. ISSN: 0945-053X.
AB The inability to study appropriate human tissues at various stages of development has precluded the elaboration of a thorough understanding of the pathogenic mechanisms leading to diseases linked to mutations in genes for elastic fiber proteins. Recently, new insights have been gained by studying **mice** harboring targeted mutations in the genes that encode fibrillin-1 and elastin. These genes have been linked to Marfan syndrome (MFS) and supravalvular aortic stenosis (SVAS), respectively. For fibrillin-1, **mouse** models have revealed that phenotype is determined by the degree of functional impairment. The haploinsufficiency state or the expression of low levels of a product with dominant-negative potential from one allele is associated with mild phenotypes with a predominance of skeletal features. Exuberant expression of a

dominant-negative-acting protein leads to the more severe MFS phenotype. **Mice** harboring targeted **deletion** of the **elastin** gene (ELN) show many of the features of SVAS in humans, including abnormalities in the vascular wall and altered hemodynamics associated with changes in wall compliance. The genetically altered **mice** suggest that SVAS is predominantly a disease of haploinsufficiency. These studies have underscored the prominent role of the elastic matrix in the morphogenesis and homeostasis of the vessel wall.

L4 ANSWER 9 OF 85 MEDLINE DUPLICATE 7
AU de Luis O; Valero M C; Jurado L A
TI WBSCR14, a putative transcription factor gene deleted in Williams-Beuren syndrome: complete characterisation of the human gene and the mouse ortholog.
SO EUROPEAN JOURNAL OF HUMAN GENETICS, (2000 Mar) 8 (3) 215-22.
Journal code: 9302235. ISSN: 1018-4813.
AB Williams-Beuren syndrome (WBS) is a neurodevelopmental disorder affecting several systems caused by a heterozygous deletion in the chromosomal region 7q11.23. A common interval that includes up to 17 genes reported so far is **deleted** in the great majority of patients. **Elastin** haploinsufficiency is responsible for the cardiovascular features, but the specific contribution of other deleted genes to the WBS phenotype remains unknown. We have fully characterised a gene commonly deleted in WBS, WBSCR14, previously reported in a truncated form as WS-bHLH. The WBSCR14 cDNA encodes an 852amino acid protein with a basic helix-loop-helix-leucine-zipper motif (bHLHZip) and a bipartite nuclear localisation signal (BNLS), suggesting a function as a transcription factor. WBSCR14 is expressed as a 4.2kb transcript predominantly in adult liver and at late stages of foetal development. The WBSCR14 locus encompasses 33 kb of genomic DNA with 17 exons. Two intragenic polymorphic dinucleotide repeats have been identified and used to verify hemizygosity in WBS patients. We have also cloned the **mouse** ortholog and mapped its locus to **mouse** chromosome 5, in a region of conserved synteny with human 7q11.23. Given that other bHLHZip proteins are dosage sensitive and based on the putative function of WBSCR14 as a transcription factor, hemizygosity at this locus could be involved in some features of WBS.

L4 ANSWER 10 OF 85 BIOSIS COPYRIGHT 2003 BIOLOGICAL ABSTRACTS INC.
AU Lijnen, H. R. (1)
TI Molecular interactions between the plasminogen/plasmin and matrix metalloproteinase systems.
SO Fibrinolysis & Proteolysis, (March May, 2000) Vol. 14, No. 2-3, pp. 175-181. print.
ISSN: 1369-0191.
AB Circumstantial evidence suggests an important role of the fibrinolytic (plasminogen/plasmin) and matrix metalloproteinase (MMP) systems in biological processes involving (extra)cellular proteolysis and matrix degradation. The availability of **mice** with inactivation of main components of both systems has allowed to study directly the interactions between both systems and their biological role. In purified system, MMP-3 (stromelysin-1) specifically hydrolyzes plasminogen and urokinase-type plasminogen activator (u-PA), thereby removing the cellular binding domains from both proteins. In the presence of cells, MMP-3 may downregulate cell-associated plasmin activity by decreasing the amount of activatible plasminogen, without affecting cell-bound u-PA activity. During neointima formation after vascular injury in gene-deficient **mice**, expression of MMP-2 and MMP-9 (gelatinase A and B) is strongly enhanced, independently of the presence or absence of plasminogen or of the physiological plasminogen activators. Activation of proMMP-2 occurs independently of plasmin, whereas proMMP-9 activation occurs via plasmin-dependent as well as plasmin-independent mechanisms. The temporal and topographic expression patterns of MMP-2, MMP-3, MMP-9, MMP-12 (metalloelastase) and MMP-13 (collagenase) establish a potential role in

neointima formation. This is further substantiated by the finding that neointima formation after vascular injury is significantly enhanced in **mice** with deficiency of TIMP-1, a main physiological MMP inhibitor. Atherosclerosis models in gene-deficient **mice** suggest an important role of u-PA in the structural integrity of the atherosclerotic vessel wall. u-PA-mediated plasmin generation may contribute to activation of latent MMPs (MMP-3, -9, -12, and -13) which degrade insoluble **elastin** and fibrillar collagen. Thus, studies with gene-**deficient mice** have allowed to establish novel interactions between the fibrinolytic and MMP systems, which may play a role in biological processes requiring cellular proteolytic activity and/or extracellular matrix degradation.

L4 ANSWER 11 OF 85 MEDLINE DUPLICATE 8
AU McGowan S; Jackson S K; Jenkins-Moore M; Dai H H; Chambon P; Snyder J M
TI **Mice** bearing **deletions** of retinoic acid receptors demonstrate reduced lung **elastin** and alveolar numbers.
SO AMERICAN JOURNAL OF RESPIRATORY CELL AND MOLECULAR BIOLOGY, (2000 Aug) 23 (2) 162-7.
Journal code: 8917225. ISSN: 1044-1549.
AB In mammals, including rats and mice, the development of pulmonary alveolar septa is primarily limited to late gestation and the early periods of postnatal life. Before this time, the rat lung contains a relatively large supply of endogenous retinyl ester that, together with its metabolite retinoic acid, has been shown to increase elastin gene expression and the number of alveoli. We have hypothesized that mice bearing a deletion of one or more genes encoding for retinoic acid receptors (which are DNA binding proteins that alter transcription of retinoic acid-responsive genes) may demonstrate abnormalities in retinoid-mediated alveolar formation. Our studies demonstrate that the absence of the retinoic acid receptor-gamma (RARgamma) is associated with a decrease in the steady-state level of tropoelastin messenger RNA in a subpopulation of lung fibroblasts at Postnatal Day 12. RARgamma gene deletion also resulted in a decrease in whole lung elastic tissue and alveolar number, and an increase in mean cord length of alveoli (L(m)) at Postnatal Day 28. The additional deletion of one retinoid X receptor (RXR)alpha allele resulted in a decrease in alveolar surface area and alveolar number, and an increase in L (m). These data indicate that RARgamma is required for the formation of normal alveoli and alveolar elastic fibers in the mouse, and that RAR/RXR heterodimers are involved in alveolar morphogenesis.

L4 ANSWER 12 OF 85 MEDLINE DUPLICATE 9
AU Peoples R; Franke Y; Wang Y K; Perez-Jurado L; Paperna T; Cisco M; Francke U
TI A physical map, including a BAC/PAC clone contig, of the Williams-Beuren syndrome--deletion region at 7q11.23.
SO AMERICAN JOURNAL OF HUMAN GENETICS, (2000 Jan) 66 (1) 47-68.
Journal code: 0370475. ISSN: 0002-9297.
AB Williams-Beuren syndrome (WBS) is a developmental disorder caused by haploinsufficiency for genes in a 2-cM region of chromosome band 7q11.23. With the exception of vascular stenoses due to **deletion** of the **elastin** gene, the various features of WBS have not yet been attributed to specific genes. Although >/=16 genes have been identified within the WBS deletion, completion of a physical map of the region has been difficult because of the large duplicated regions flanking the deletion. We present a physical map of the WBS deletion and flanking regions, based on assembly of a bacterial artificial chromosome/P1-derived artificial chromosome contig, analysis of high-throughput genome-sequence data, and long-range restriction mapping of genomic and cloned DNA by pulsed-field gel electrophoresis. Our map encompasses 3 Mb, including 1.6 Mb within the deletion. Two large duplicons, flanking the deletion, of >/=320 kb contain unique sequence elements from the internal border regions of the deletion, such as sequences from GTF2I (telomeric) and FKBP6 (centromeric). A third copy of this duplicon exists in inverted

orientation distal to the telomeric flanking one. These duplicons show stronger sequence conservation with regard to each other than to the presumptive ancestral loci within the common deletion region. Sequence elements originating from beyond 7q11.23 are also present in these duplicons. Although the duplicons are not present in **mice**, the order of the single-copy genes in the conserved syntenic region of **mouse** chromosome 5 is inverted relative to the human map. A model is presented for a mechanism of WBS-deletion formation, based on the orientation of duplicons' components relative to each other and to the ancestral elements within the deletion region.

L4 ANSWER 13 OF 85 MEDLINE DUPLICATE 10
AU Faury G; Maher G M; Li D Y; Keating M T; Mecham R P; Boyle W A
TI Relation between outer and luminal diameter in cannulated arteries.
SO AMERICAN JOURNAL OF PHYSIOLOGY, (1999 Nov) 277 (5 Pt 2) H1745-53.
Journal code: 0370511. ISSN: 0002-9513.
AB Resistance in blood vessels is directly related to the inner (luminal) diameter (ID). However, ID can be difficult to measure during physiological experiments because of poor transillumination of thick-walled or tightly constricted vessels. We investigated whether the wall cross-sectional area (WCSA) in cannulated arteries is nearly constant, allowing IDs to be calculated from outer diameters (OD) using a single determination of WCSA. With the use of image analysis, OD and ID were directly measured using either transillumination or a fluorescent marker in the lumen. IDs from a variety of vessel types were calculated from WCSA at several reference pressures. Calculated IDs at all of the reference WCSA were within 5% (mean <1%) of the corresponding measured IDs in all vessel types studied, including vessels from heterozygote **elastin knockout animals**. This was true over a wide range of transmural pressures, during treatment with agonists, and before and after treatment with KCN. In conclusion, WCSA remains virtually constant in cannulated vessels, allowing accurate determination of ID from OD measurement under a variety of experimental conditions.

L4 ANSWER 14 OF 85 CAPLUS COPYRIGHT 2003 ACS
AU Zhang, Jun; Kumar, Anil; Roux, Kyle; Williams, Charles A.; Wallace, Margaret R.
TI Elastin region deletions in Williams syndrome
SO Genetic Testing (1999), 3(4), 357-359
CODEN: GETEF4; ISSN: 1090-6576
AB Williams syndrome (WS) is considered a contiguous gene syndrome, with most patients having a 1.5-Mb deletion of chromosome 7q11.23 contg. the elastin gene and flanking genes. Studies of the frequency, extent, and origin of these deletions are ongoing in many labs to discover ultimately the mol. and pathogenetic basis for WS. An anal. of 9 sporadic WS families with typical phenotypes was performed by genotyping polymorphisms in the region. This study revealed deletions in all 9 patients, with 1 showing a novel deletion extending much further centromeric than any other WS deletions yet reported.

L4 ANSWER 15 OF 85 CAPLUS COPYRIGHT 2003 ACS
AU Wu, Wendy J.; Weiss, Anthony S.
TI Deficient coacervation of two forms of human tropoelastin associated with supravalvular aortic stenosis
SO European Journal of Biochemistry (1999), 266(1), 308-314
CODEN: EJBCAI; ISSN: 0014-2956
AB Human tropoelastin assocs. by coacervation and is subsequently cross-linked to make elastin. In Williams syndrome, defective elastin deposition is assocd. with hemizygous deletion of the tropoelastin gene in supravalvular aortic stenosis (SVAS). Remarkably, point-mutation forms of SVAS correspond to incomplete forms of tropoelastin which include in-frame termination by nonsense mutations, yet the resulting phenotype of these disorders is not explained because expression variably occurs from both normal and mutant alleles. Proteins corresponding to two truncated

tropoelastin mutants were expressed and purified to homogeneity. Coacervation of these proteins occurred as expected with increasing temp., but substantially contrasted with that of the performance of a normal tropoelastin. Significantly, assocn. by coacervation of the truncated SVAS tropoelastin mols. was negligible at 37.degree., which contrasted with the substantial coacervation seen for normal tropoelastin. Furthermore their midpoints of coacervation increased and correlated with the extent of deletion, in accord with the loss of hydrophobic regions required for tropoelastin assocn. Their secondary structures are similar, as evidenced by CD studies. We propose a model for point-mutation SVAS in which aberrant tropoelastin mols. are incompetent and are mainly excluded from participation in coacervation and consequently in elastogenesis. These forms of SVAS may consequently be considered functionally similar to a hemizygous deletion, and mark point-mutation SVAS as a disorder of defective coacervation.

L4 ANSWER 16 OF 85 MEDLINE DUPLICATE 11
AU Mahmoodian F; Peterkofsky B
TI Vitamin C deficiency in guinea pigs differentially affects the expression of type IV collagen, laminin, and elastin in blood vessels.
SO JOURNAL OF NUTRITION, (1999 Jan) 129 (1) 83-91.
Journal code: 0404243. ISSN: 0022-3166.
AB Vitamin C deficiency causes morphologic changes in the endothelial and smooth muscle compartments of guinea **pig** blood vessels. Endothelial cells synthesize the basement membrane components, type IV collagen and laminin, and smooth muscle cells synthesize elastin in blood vessels. Therefore, we examined the possibility that vitamin C deficiency affects the expression of these proteins. Decreased expression of types I and II collagens in other tissues of vitamin C-deficient guinea **pigs** is associated with weight loss and the consequent induction of insulin-like growth factor binding proteins; thus we also used food deprivation to induce weight loss. Female guinea **pigs** received a vitamin C-free diet, supplemented orally with ascorbate. Vitamin C-deficient guinea **pigs** received the same diet but no ascorbate, and the food-deprived group received no food, but were supplemented with vitamin C. Concentrations of mRNAs for basement membrane components and elastin in blood vessels were measured by Northern blotting; overall basement membrane metabolism was assessed by measuring immunoreactive laminin and type IV 7S collagen in serum. Laminin mRNA in blood vessels and serum laminin concentrations were unaffected by vitamin C **deficiency**. Concentrations of type IV collagen and **elastin** mRNAs in blood vessels were not significantly affected in moderately scorbutic guinea **pigs** (0-7% weight loss), but with increased weight loss, type IV collagen mRNA was 57% (P < 0.05) and elastin mRNA was 3% (P < 0. 01) of normal values. In food-deprived guinea **pigs**, type IV collagen mRNA was 51% (P < 0.05) and elastin mRNA was 35% (P < 0.05) of normal. Serum type IV 7S collagen concentrations were 25% of normal in scorbutic guinea **pigs** with extensive weight loss. The lower expression of type IV collagen and elastin mRNAs in blood vessels may contribute to defects observed in blood vessels during scurvy.

L4 ANSWER 17 OF 85 CAPLUS COPYRIGHT 2003 ACS
AU Antipatis, Christos; Ashworth, Cheryl J.; Grant, George; Lea, Richard G.; Hay, Susan M.; Rees, William D.
TI Effects of maternal vitamin A status on fetal heart and lung: changes in expression of key developmental genes
SO American Journal of Physiology (1998), 275(6, Pt. 1), L1184-L1191
CODEN: AJPHAP; ISSN: 0002-9513
AB Vitamin A is required for fetal lung development during pregnancy. These expts. monitored fetal lung morphol. in normal and vitamin A-deficient rats. The expression of elastin and the growth arrest-specific gene 6 (gas6) in fetal and neonatal hearts and lungs was assessed by Northern blotting. In normal rats, elastin and gas6 were expressed in the fetal lung and heart from day 19 of gestation up to postnatal day 2. Maternal

vitamin A deficiency altered the fetal lung development. On day 20, the bronchial passageways were less developed and showed decreased staining for elastic fibers; in neonates the relative air space and the size of the sacculi were decreased. In the fetal lung, the mRNAs for elastin and gas6 were decreased to 56 and 68% of the control values, resp. In the fetal heart, the mRNA for elastin was decreased to 64% of the control value, whereas gas6 was increased 2-fold. In the neonate, there was no change in the elastin expression in the lung or heart, but the gas6 expression in the heart was increased 2-fold. Thus, in the pregnant rat, vitamin A deficiency may retard fetal lung development or influence the differentiation of crit. cell lines. The changes in elastin and gas6 expression may be used to identify the cell types affected.

L4 ANSWER 18 OF 85 CAPLUS COPYRIGHT 2003 ACS
AU Martorana, Piero A.; Lungarella, Giuseppe
TI Genetic deficiency in .alpha.1 proteinase inhibitor (.alpha.1 PI) associated with emphysema
SO Laboratory Animal Science (1998), 48(5), 460-462
CODEN: LBASAE; ISSN: 0023-6764
AB The authors report a severe genetic deficiency of serum .alpha.1-proteinase inhibitor (.alpha.1 PI) assocd. with low serum anti-elastase screen in the pallid (pa) mouse, a strain with spontaneously occurring emphysema. This appears to be the 1st animal model in which a direct sequence of events consists of serum deficiency of anti-elastase screen, increased elastase burden on lung elastin, decreased elastin content in the lungs and anat. emphysema.

L4 ANSWER 19 OF 85 MEDLINE DUPLICATE 12
AU Morris C A
TI Genetic aspects of supravalvular aortic stenosis.
SO CURRENT OPINION IN CARDIOLOGY, (1998 May) 13 (3) 214-9. Ref: 56
Journal code: 8608087. ISSN: 0268-4705.
AB Supravalvular aortic stenosis (SVAS) occurs as an autosomal dominant trait or as part of the phenotype of the usually sporadic condition Williams syndrome. SVAS is the result of mutation or **deletion** of the **elastin** gene (ELN), located at chromosome 7q11.23. Thus, SVAS may be more appropriately termed an elastin arteriopathy. Studies have demonstrated various point mutations and intragenic deletions of ELN resulting in nonsyndromic SVAS. Individuals with Williams syndrome are hemizygous for the **elastin** gene, owing to a 1 to 2 megabase **deletion** of a portion of the long arm of chromosome 7 that encompasses ELN. This submicroscopic deletion is readily detected by fluorescent in-situ hybridization, useful in the diagnosis of Williams syndrome. The severity of SVAS is quite variable, both in series of Williams syndrome patients and within SVAS kindreds, suggesting that other genetic factors are involved in expression of the phenotype. Experiments with **elastin knockout mice** will likely yield clues regarding the role of elastin in arterial morphogenesis and the pathogenesis of obstructive vascular disease.

L4 ANSWER 20 OF 85 CAPLUS COPYRIGHT 2003 ACS
AU Lindahl, Per; Karlsson, Linda; Hellstrom, Mats; Gebre-Medhin, Samuel; Willetts, Karen; Heath, John K.; Betsholtz, Christer
TI Alveogenesis failure in PDGF-A-deficient mice is coupled to lack of distal spreading of alveolar smooth muscle cell progenitors during lung development
SO Development (Cambridge, United Kingdom) (1997), 124(20), 3943-3953
CODEN: DEVPED; ISSN: 0950-1991
AB PDGF-A-/- mice lack lung alveolar smooth muscle cells (SMC), exhibit reduced deposition of elastin fibers in the lung parenchyma, and develop lung emphysema due to complete failure of alveogenesis. The authors have mapped the expression of PDGF-A, PDGF receptor-.alpha., tropoelastin, smooth muscle .alpha.-actin and desmin in developing lungs from wild type and PDGF-A-/- mice of pre- and postnatal ages to get insight into the

mechanisms of PDGF-A-induced alveolar SMC formation and elastin deposition. PDGF-A was expressed by developing lung epithelium. Clusters of PDGF-R.alpha.-pos. (PDGF-R.alpha.+) mesenchymal cells occurred at the distal epithelial branches until embryonic day (E) 15.5. Between E16.5 and E17.5, PDGF-R.alpha.+ cells multiplied and spread to acquire positions as solitary cells in the terminal sac walls, where they remained until the onset of alveogenesis. In PDGF-A-/- lungs PDGF-R.alpha.+ cells failed to multiply and spread and instead remained in prospective bronchiolar walls. Three phases of tropoelastin expression were seen in the developing lung, each phase characterized by a distinct pattern of expression. The third phase, tropoelastin expression by developing alveolar SMC in conjunction with alveogenesis, was specifically and completely absent in PDGF-A-/- lungs. The authors propose that lung PDGF-R.alpha.+ cells are progenitors of the tropoelastin-pos. alveolar SMC. The authors also propose that postnatal alveogenesis failure in PDGF-A-/- mice is due to a prenatal block in the distal spreading of PDGF-R.alpha.+ cells along the tubular lung epithelium during the canalicular stage of lung development.

L4 ANSWER 21 OF 85 CAPLUS COPYRIGHT 2003 ACS
AU Jaeken, Jaak; Detheux, Michel; Fryns, Jean-Pierre; Collet, Jean-Francois; Alliet, Philippe; Van Schaftingen, Emile
TI Phosphoserine phosphatase deficiency in a patient with Williams syndrome
SO Journal of Medical Genetics (1997), 34(7), 594-596
CODEN: JMDGAE; ISSN: 0022-2593
AB Decreased serine levels were found in plasma and cerebrospinal fluid (CSF) of a boy with pre- and postnatal growth retardation, moderate psychomotor retardation, and facial dysmorphism suggestive of Williams syndrome. Fluorescence in situ hybridization with an elastin gene probe indicated the presence of a submicroscopic 7q11.23 deletion, confirming this diagnosis. Further investigation showed that the phosphoserine phosphatase (EC 3.1.3.3.) activity in lymphoblasts and fibroblasts amounted to about 25% of normal values. Oral serine normalized the plasma and CSF levels of this amino acid and seemed to have some clin. effect. These data suggest that the elastin gene and the phosphoserine phosphatase gene might be closely linked. This seems to be the first report of phosphoserine phosphatase deficiency.

L4 ANSWER 22 OF 85 MEDLINE DUPLICATE 13
AU Paik D C; Ramey W G; Dillon J; Tilson M D
TI The nitrite/elastin reaction: implications for in vivo degenerative effects.
SO CONNECTIVE TISSUE RESEARCH, (1997) 36 (3) 241-51.
Journal code: 0365263. ISSN: 0300-8207.
AB Nitrite ion is a by-product of nitrogen oxides (nitric oxide and nitrogen dioxide) from cigarette smoke and is used as a preservative for curing meats. Therefore, study of the reaction of nitrite with elastin in vitro was undertaken. By colorimetric assay, reactivity of nitrite with insoluble elastin at neutral pH, 37 degrees C, and physiologic concentration was confirmed. In histochemical studies on in situ human aortic elastin, nitrite-treated sections displayed marked structural disruptions. Determinations of fluorescence and absorbance on nitrite-treated soluble **bovine** elastin revealed marked alterations of fluorescence, and increased UV and visible absorbance. Amino acid analysis confirmed that it reacted with tyrosine. The findings indicate that non-enzymatic nitration by nitrite may have **deleterious** effects on **elastin** in vivo and may provide insights into the pathogenesis of chronic elastin degenerative processes, including aortic aneurysms, pulmonary emphysema, and premature skin wrinkling, all of which have been well known to have associations with cigarette smoking.

L4 ANSWER 23 OF 85 CAPLUS COPYRIGHT 2003 ACS
AU Dutly, Fabrizio; Schinzel, Albert
TI Unequal interchromosomal rearrangements may result in elastin gene

deletions causing the Williams-Beuren syndrome
SO Human Molecular Genetics (1996), 5(12), 1893-1898
CODEN: HMGEE5; ISSN: 0964-6906
AB Williams-Beuren syndrome (WBS) is generally the consequence of an interstitial microdeletion at 7q11.23, which includes the elastin gene, thus causing hemizygosity at the elastin gene locus. The origin of the deletion has been reported by many authors to be maternal in .apprx.60% and paternal in 40% of cases. Segregation anal. of grandpaternal markers flanking the microdeletion region in WBS patients and their parents indicated that in the majority of cases a recombination between grandmaternal and grandpaternal chromosomes 7 at the site of the deletion had occurred during meiosis in the parent from whom the deleted chromosome stemmed. Thus, the majority of deletions were considered a consequence of unequal crossing-over between homologous chromosomes 7 (interchromosomal rearrangement) while the remaining cases an intrachromosomal recombination (between the chromatids of one chromosome 7) may have occurred. These results suggest that the majority of interstitial deletions of the elastin gene region occur during meiosis, due to unbalanced recombination while a minority could occur before or during meiosis probably due to intrachromosomal rearrangements. The recurrence risk of the interchromosomal rearrangements for sibs of a proband with non-affected parents must be negligible, which fits well with the observation of sporadic occurrence of almost all cases of WBS.

L4 ANSWER 24 OF 85 CAPLUS COPYRIGHT 2003 ACS
AU Jurado, Luis A. Perez; Peoples, Risa; Kaplan, Paige; Hamel, Ben C. J.; Francke, Uta
TI Molecular definition of the chromosome 7 deletion in Williams syndrome and parent-of-origin effects on growth
SO American Journal of Human Genetics (1996), 59(4), 781-792
CODEN: AJHGAG; ISSN: 0002-9297
AB Williams syndrome (WS) is a developmental disorder with variable phenotypic expression assocd., in most cases, with a hemizygous deletion of part of chromosomal band 7q11.23 that includes the elastin gene (ELN). The authors have investigated the frequency and size of the deletions, detd. the parental origin, and correlated the mol. results with the clin. findings in 65 WS patients. Hemizygosity at the ELN locus was established by typing of two intragenic polymorphisms, quant. Southern anal., and/or FISH. Polymorphic markers covering the deletion and flanking regions were ordered by a combination of genetic and phys. mapping. Genotyping of WS patients and available parents for 13 polymorphisms revealed that of 65 clin. defined WS patients, 61 (94%) had a deletion of the ELN locus and were also hemizygous (or non-informative) at loci D7S489B, D7S2476, D7S613, D7S2472, and D7S1870. None of the four patients without ELN deletion was hemizygous at any of the polymorphic loci studied. All patients were heterozygous (or noninformative) for centromeric (D7S1816, D7S1483, and D7S653) and telomeric (D7S489A, D7S675, and D7S669) flanking loci. The genetic distance between the most-centromeric deleted locus, D7S489B, and the most-telomeric one, D7S1870, is 2 cM. The breakpoints cluster at .apprx.1 cM to either side of ELN. In 39 families informative for parental origin, all deletions were de novo, and 18 were paternally and 21 maternally derived. Comparison of clin. data, collected in a standardized quantifiable format, revealed significantly more severe growth retardation and microcephaly in the maternal deletion group. An imprinted locus, silent on the paternal chromosome and contributing to statural growth, may be affected by the deletion.

L4 ANSWER 25 OF 85 MEDLINE DUPLICATE 14
AU Cavarra E; Martorana P A; Gambelli F; de Santi M; van Even P; Lungarella G
TI Neutrophil recruitment into the lungs is associated with increased lung elastase burden, decreased lung **elastin**, and emphysema in alpha 1 proteinase inhibitor-**deficient mice**.
SO LABORATORY INVESTIGATION, (1996 Aug) 75 (2) 273-80.
Journal code: 0376617. ISSN: 0023-6837.

AB The possibility that polymorphonuclear leukocytes (PMN) recruited into the lung have the capability to damage alveolar septa was investigated in several strains of mice with different serum alpha 1 proteinase inhibitor levels and PMN lysosomal functions. After an intratracheal instillation of FMLP (200 micrograms), all strains of mice showed a similar PMN influx in alveolar spaces with an increase (approximately 4- to 5-fold) in bronchoalveolar lavage total cell count, which peaked at 24 to 48 hours. At this time, differential cell count in all strains revealed an approximately 40-fold increase in neutrophils. In C57BL/6J and pallid mice but not in NMRI mice, PMN influx was followed by a decrease in lung elastin content (-17% and -37%, respectively) and by the development of significant emphysema (mean linear intercept, +28% and +56%, respectively). The onset of the pulmonary lesion was preceded by a marked increase of neutrophil elastase burden in alveolar interstitium. Compared with NMRI mice, C57BL/6J and pallid mice have lower serum elastase inhibitory capacity levels. The degree of lung destruction was inversely correlated with elastase inhibitory capacity levels. Lung elastin degradation and emphysema may be induced by eliciting PMN into the lungs only in animals with a deficient anti-elastase screen. Compared with C57BL/6J mice, pallid mice showed a significantly greater lung elastin loss and a higher degree of emphysema after FMLP treatment. These differences may be accounted for by the higher baseline levels of interstitial elastase burden. It may be assumed that an enzymatically active elastase was already working on the lung interstitium before FMLP instillation in pallid mice.

L4 ANSWER 26 OF 85 CAPLUS COPYRIGHT 2003 ACS
AU Frangiskakis, J. Michael; Ewart, Amanda K.; Morris, Colleen A.; Mervis, Carolyn B.; Bertrand, Jacquelyn; Robinson, Byron F.; Klein, Bonita P.; Ensing, Gregory J.; Everett, Lorraine A.; et al.
TI LIM-kinase1 hemizygosity implicated in impaired visuospatial constructive cognition
SO Cell (Cambridge, Massachusetts) (1996), 86(1), 59-69
CODEN: CELLB5; ISSN: 0092-8674
AB To identify genes important for human cognitive development, the authors studied Williams syndrome (WS), a developmental disorder that includes poor visuospatial constructive cognition. Here the authors describe two families with a partial WS phenotype; affected members have the specific WS cognitive profile and vascular disease, but lack other WS features. Submicroscopic chromosome 7q11.23 deletions co-segregate with this phenotype in both families. DNA sequence analyses of the region affected by the smallest deletion (83.6 kb) revealed two genes, elastin (ELN) and LIM-kinase1 (LIMK1). The latter encodes a novel protein kinase with LIM domains and is strongly expressed in the brain. Because ELN mutations cause vascular disease but not cognitive abnormalities, these data implicate LIMK1 hemizygosity in impaired visuospatial constructive cognition.

L4 ANSWER 27 OF 85 CAPLUS COPYRIGHT 2003 ACS
AU Robinson, W. P.; Waslynka, J.; Bernasconi, F.; Wang, M.; Clark, S.; Kotzot, D.; Schinzel, A.
TI Delineation of 7q11.2 deletions associated with Williams-Beuren syndrome and mapping of a repetitive sequence to within and to either side of the common deletion
SO Genomics (1996), 34(1), 17-23
CODEN: GNMCEP; ISSN: 0888-7543
AB The majority of Williams-Beuren syndrome (WBS) patients have been shown to have a microdeletion within 7q11.2 including the elastin gene locus. The extent of these deletions has, however, not been well characterized. Thirty-five deletion patients were tested for all polymorphic markers in the 7q11.2 region bounding ELN to define the extent of deletions assocd. with WBS. With only one exception, ELN, D7S1870, and one copy of the D7S489 locus (D7S489U) were always included in the deletions. One patient showed lack of maternal inheritance at D7S1870 and not at ELN or D7S489U.

A product corresponding to D7S489U was amplified from YAC 743G6 and from the P1 clone RMC07P008, thereby localizing both to within the common deletion. The boundary of the deleted region on the proximal (centromeric) side is D7S653 and on the distal side is D7S675, neither of which were ever included in the deletion. One locus, D7S489L, was variably deleted in patients, indicating a min. of two common breakpoints on the proximal side. At least one addnl. repeat amplified by D7S489 (D7S489M) was localized to a YAC contig mapping distal to the common deletion. The D7S489 sequence is highly homologous to several cDNA clones in the GenBank database and contains an Alu sequence. It is possible that this and/or other repetitive sequences in this region could play a role in the mechanism of deletion.

L4 ANSWER 28 OF 85 CAPLUS COPYRIGHT 2003 ACS
AU Olson, Timothy M.; Michels, Virginia V.; Urban, Zsolt; Csiszar, Katalin; Christiano, Angela M.; Driscoll, David J.; Feldt, Robert H.; Boyd, Charles D.; Thibodeau, Stephen N.
TI A 30 kb deletion within the elastin gene results in familial supravalvular aortic stenosis
SO Human Molecular Genetics (1995), 4(9), 1677-9
CODEN: HMGEE5; ISSN: 0964-6906
AB Supravalvular aortic stenosis (SVAS) is a congenital vascular disorder that has been linked to the elastin gene. Southern blot anal. was used to screen for mutations within the elastin gene in 6 familial and 3 sporadic cases of SVAS without features of Williams syndrome. An elastin gene deletion was identified in one of these cases. The deletion was found in a proband and his mother in a Middle Eastern family. It was an approx. 30-kb deletion involving exons 2-27 with breakpoints in intron 1 and between EcoRI and BamHI restriction sites in intron 27. PCR amplification of genomic DNA and sequencing localized the breakpoints within 2 AluI-repeat sequences, 1800 bp 3' of exon 1 and 500 bp 5' of exon 28, creating a chimeric intron of 2.3 kb.

L4 ANSWER 29 OF 85 CAPLUS COPYRIGHT 2003 ACS
AU Mari, A; Amati, F.; Mingarelli, R.; Giannotti, A.; Sebastio, G.; Colloridi, V.; Novelli, G.; Dallapiccola, B.
TI Analysis of the elastin gene in 60 patients with clinical diagnosis of Williams syndrome
SO Human Genetics (1995), 96(4), 444-8
CODEN: HUGEDQ; ISSN: 0340-6717
AB Williams syndrome (WS) is caused by deletion of the elastin (ELN) gene. The authors have analyzed an intragenic restriction fragment length polymorphism (RFLP) and the gene dosage of ELN using a new probe (FP4) in a series of 60 sporadic patients with a clin. diagnosis of WS. Deletion of the ELN gene was shown in 54 cases, while clin. revaluation of the 6 patients without the deletion did not confirm the diagnosis of WS. These results support the genetic homogeneity of WS, and the high accuracy of ELN mol. anal., which can be confidently used for providing genetic counseling to WS families.

=>

STIC-ILL

From: Chen, Shin-Lin
Sent: Wednesday, January 15, 2003 6:10 PM
To: STIC-ILL
Subject: articles

Please provide the following articles ASAP. thanks!
Serial No. 09/258,217.

L4 ANSWER 28 OF 85 CAPLUS COPYRIGHT 2003 ACS
AU Olson, Timothy M.; Michels, Virginia V.; Urban, Zsolt; Csiszar, Katalin; Christiano, Angela M.; Driscoll, David J.; Feldt, Robert H.; Boyd, Charles D.; Thibodeau, Stephen N.
TI A 30 kb deletion within the elastin gene results in familial supravalvular aortic stenosis
SO Human Molecular Genetics (1995), 4(9), 1677-9
CODEN: HMGEE5; ISSN: 0964-6906

L4 ANSWER 29 OF 85 CAPLUS COPYRIGHT 2003 ACS
AU Mari, A; Amati, F.; Mingarelli, R.; Giannotti, A.; Sebastio, G.; Colloridi, V.; Novelli, G.; Dallapiccola, B.
TI Analysis of the elastin gene in 60 patients with clinical diagnosis of Williams syndrome
SO Human Genetics (1995), 96(4), 444-8.

L4 ANSWER 20 OF 85 CAPLUS COPYRIGHT 2003 ACS
AU Lindahl, Per; Karlsson, Linda; Hellstrom, Mats; Gebre-Medhin, Samuel; Willetts, Karen; Heath, John K.; Betsholtz, Christer
TI Alveogenesis failure in PDGF-A-deficient mice is coupled to lack of distal spreading of alveolar smooth muscle cell progenitors during lung development
SO Development (Cambridge, United Kingdom) (1997), 124(20), 3943-3953.

L4 ANSWER 40 OF 85 CAPLUS COPYRIGHT 2003 ACS
AU Ewart, Amanda K.; Morris, Colleen A.; Atkinson, Donald; Jin, Weishan; Sternes, Keith; Spallone, Patricia; Stock, A. Dean; Leppert, Mark; Keating, Mark T.
TI Hemizygosity at the elastin locus in a developmental disorder, Williams syndrome
SO Nature Genetics (1993), 5(1), 11-16.

L4 ANSWER 31 OF 85 CAPLUS COPYRIGHT 2003 ACS
AU Dallapiccola, B.; Amati, F.; Gennarelli, M.; Mari, A.; Novelli, G.
TI Advances in molecular analysis of congenital heart defects.
SO Bulletin of Molecular Biology and Medicine (1995), 20(3,4), 135-140.

Shin-Lin Chen
AU 1632
CM1 12A15
Mail Box: CM1 12E12
(703) 305-1678

Hemizygosity at the elastin locus in a developmental disorder, Williams syndrome

Amanda K. Ewart[1], Colleen A. Morris[5,7], Donald Atkinson[1], Weishan Jin[1], Keith Sternes[6], Patricia Spallone[8], A. Dean Stock[7,8], Mark Leppert[1,3] & Mark T. Keating[1,2,4]

Williams syndrome (WS) is a developmental disorder affecting connective tissue and the central nervous system. A common feature of WS, supravalvular aortic stenosis, is also a distinct autosomal dominant disorder caused by mutations in the elastin gene. In this study, we identified hemizygosity at the elastin locus using genetic analyses in four familial and five sporadic cases of WS. Fluorescent *in situ* hybridization and quantitative Southern analyses confirmed these findings, demonstrating inherited and *de novo* deletions of the elastin gene. These data indicate that deletions involving one elastin allele cause WS and implicate elastin hemizygosity in the pathogenesis of the disease.

[1]Department of Human Genetics, Cardiology Division[2], Howard Hughes Medical Institute[3] and Eccles Program in Human Molecular Biology and Genetics[4], University of Utah, Salt Lake City, Utah 84112, USA
[5]Department of Pediatrics, University of Nevada School of Medicine, Las Vegas, Nevada 89102, USA
[6]Department of Microbiology and Department of Pathology and Laboratory Medicine[7], Genetics Network[8], University of Nevada School of Medicine, Reno, Nevada 89502, USA

Williams syndrome (WS) is a developmental disorder involving the vascular, connective tissue and central nervous systems[1,2]. Features of this disorder include congenital heart disease, hypertension, premature aging of skin, dysmorphic facial features (Fig. 1), infantile hypercalcemia, gregarious personality and mental retardation with IQs ranging from 20 to 106 (mean=58)[2]. The specific cognitive deficits in WS include poor visual-motor integration[2]. As a result, affected individuals have problems visualizing a complete picture but instead see only the parts. Affected individuals also suffer from attention deficit disorder. Language development, by contrast, is relatively spared and some elements of speech may be enhanced, particularly the quantity and quality of vocabulary, auditory memory, and social use of language[3,4]. Many WS patients sing or play musical instruments with considerable expertise and they rarely forget a name. The unusual neurobehavioural features of WS may be related to specific anatomical findings, particularly enlargement of neocerebellar lobules[3,4]. Because of their engaging personalities, language skills and loquaciousness, mental retardation is often underestimated in children with WS.

A common feature of WS, supravalvular aortic stenosis (SVAS), also exists as a distinct, autosomal dominant trait. SVAS is an inherited vascular disease that causes narrowing of large, elastic arteries like the aorta and pulmonary arteries[5,6]. These vascular abnormalities may require surgical correction early in life and can cause heart failure and death if untreated. The relationship between WS and SVAS was unknown until recently, when we identified linkage between the elastin gene and SVAS in two families[7]. We showed

Fig. 1 Front (*a*) and lateral (*b*) view of individual II-1 of K1998 at three years of age. The child has characteristic Williams syndrome facies including broad forehead, bitemporal narrowness, periorbital fullness, malar flattening, wide mouth, broad nasal tip, long philtrum, prominent ear lobule, full cheeks and micrognathia. The child has had other complications including inguinal hernia, supravalvular aortic stenosis which has been surgically repaired, peripheral pulmonic stenosis, radial ulnar synostosis, chronic otitis media and a hoarse voice. The child also has developmental delay and an outgoing personality typical of Williams syndrome.

Table 1 Phenotypic features of Williams Syndrome patients

Patient	K1806 II-1	K1806 III-1	K2042 I-1	K2042 II-1	K1866 II-1	K1868 II-1	K1888 II-1	K1998 II-1	K2767 II-1
Age	34	3	30	2	12	8	23	2	5
WS facial features	+	+	+	+	+	+	+	+	+
Esotropia	+	−	−	+	+	+	+	−	+
Dental malocclusion	−	+	+	+	−	+	+	−	−
Hoarse Voice	+	+	+	+	+	+	+	+	+
SVAS	−	+	−	+	+	−	+	+	+
Hernia	−	−	−	−	−	+	−	+	+
Joint limitation	+	+	+	−	−	−	+	+	−
WS personality	+	+	+	+	+	+	+	+	+
Mental retardation	+	+	+	+	+	+	+	+	+

All patients satisfy the WS diagnostic criteria[28]. Williams syndrome facial features include broad brow, bitemporal narrowing, periorbital fullness, stellate iris pattern, broad nasal tip, long smooth philtrum, flat mala, wide mouth and full cheeks.

subsequently that a chromosomal translocation cosegregating with SVAS in a third family disrupted the elastin gene, strongly suggesting that abnormalities in elastin cause this vascular disease[8]. These findings and the association between SVAS and WS led to the hypothesis that WS is a contiguous gene disorder in which the vascular and connective tissue abnormalities are caused by deletion of one elastin allele. This hypothesis is strengthened by the findings presented in this paper.

Elastin hemizygosity in familial WS

To test the hypothesis that hemizygosity at the elastin locus causes WS, we used DNA markers to screen for mutations in a rare familial case of the disorder[9]. Clinical examination of this kindred showed typical features of WS in two individuals, including SVAS, dysmorphic facial appearance, joint contractures, hernias, characteristic personality and mental retardation (Table 1). Using the elastin genomic probe, pELN5-4 (Fig. 2), in Southern analyses, a polymorphic *Pst*I fragment of 3.5 kilobases (kb) was identified in DNA samples from affected individual II-1 (Fig. 3*a*). Analysis of other family members and 240 unrelated individuals indicated that this fragment represented a rare (allele frequency of about 1%) *Pst*I polymorphism (data not shown). In DNA containing this *Pst*I site, pELN5-4 detected 2.0 and 1.5 kb fragments (allele 2); the absence of this *Pst*I site resulted in the 3.5 kb fragment (allele 1). Inspection of inheritance patterns in kindred 1806 indicated that an unaffected grandmother (individual I-2) transmitted one 3.5 kb allele to her affected child, individual II-1. This individual carried only the 3.5 kb allele, suggesting he was homozygous at this locus. However, the 3.5 kb fragment was not transmitted to this individual's affected son (individual III-1); pELN5-4 detected only the 2.0 and 1.5 kb fragments in DNA samples from this individual. These observations were not caused by false paternity as genotypic analysis using four highly polymorphic VNTR markers from other chromosomal subunits showed the expected codominant inheritance (likelihood of correct inheritance was greater than 99%; Fig. 3*b* and data not shown). These data demonstrate hemizygosity at the elastin locus in affected members of this kindred.

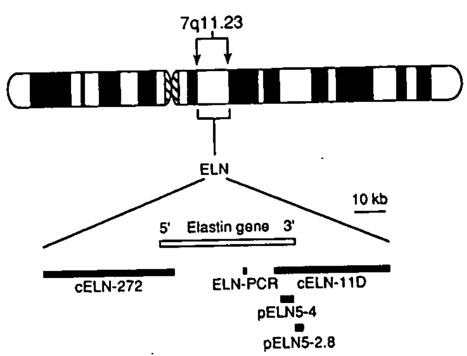

Fig. 2 Idiogram of chromosome 7 showing the location of the elastin gene which was mapped using in situ hybridization to chromosome 7q11.23 (refs 13, 23). Markers used for genotype analysis are polymorphisms within the elastin locus (ELN-*Bam*HI, ELN-*Bst*NI, ELN-*Bfa*I, ELN-*Pst*I, ELN-*Eco*RI). Elastin genomic clones (pELN5-2.8, pELN5-4)[7] and cosmids (cELN-272 and cELN-11D) are indicated.

Genotypic analyses of a second family, kindred 2402 (see Table 1), with parent to child transmission of WS showed similar results[9]. The pattern of inheritance for a polymorphism detected by elastin marker pELN5-2.8 (ref. 8) in *Eco*RI digests of DNA from this kindred also indicated non-transmission of an elastin allele from affected parent to affected child (in this case, from mother to daughter; Fig. 3*c*). Since these results were not due to misinheritance (likelihood of inheritance greater than 99%, data not shown), they indicate hemizygosity at the elastin locus in this family as well.

Elastin hemizygosity in sporadic WS

Williams syndrome is usually a sporadic disorder. To determine if hemizygosity at the elastin locus also caused sporadic WS, polymorphic elastin markers were used to screen five sporadic cases (Fig. 4*a*). Phenotypic characteristics for these cases were typical of WS (Table 1). Elastin cosmid cELN-272 (Fig. 2) detected a *Bam*HI polymorphism in kindred 1998 (Fig. 4*b*). The inheritance patterns in this family showed that the affected child (individual II-1) failed to inherit a 3.1 kb *Bam*HI fragment from his mother (individual I-1), who was homozygous for this polymorphism. Failure of maternal inheritance was also observed when a second elastin polymorphism was examined (ELN-*Eco*RI, Fig. 4*a*). The other children in this kindred showed the expected pattern of inheritance for these markers (Fig. 4). Since PCR analysis of a third elastin polymorphism (ELN-*Bfa*I)[10] showed that individual I-1 was heterozygous at the elastin locus (Fig. 4*c*), these data indicate loss of heterozygosity in the child and suggest that a *de novo* deletion involving the elastin gene caused this sporadic case of WS. Genotype analyses with polymorphic markers spanning the elastin locus revealed hemizygosity in four additional sporadic cases of WS (Fig. 4*a*). In these cases *de novo* deletions were noted in both maternal and paternal chromosomes. Misinheritance was excluded in all cases (likelihood of

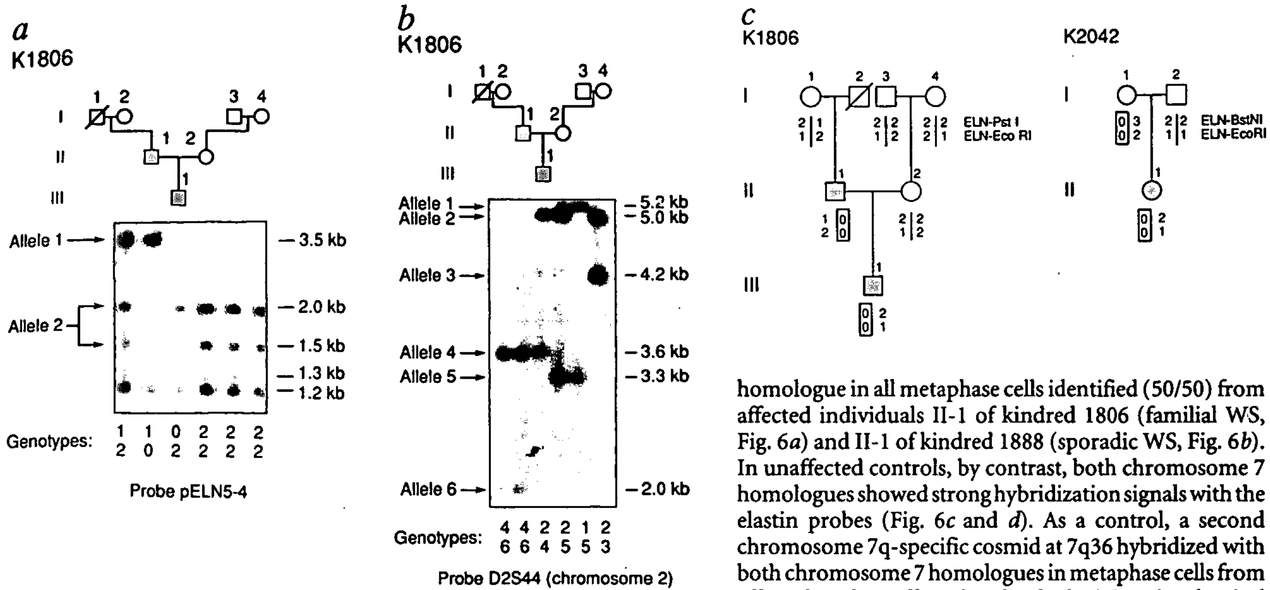

Fig. 3 Hemizygosity at the elastin locus in familial WS. *a*, Pedigree structure for familial WS kindred 1806 is shown; the phenotypic characteristics of this family have been described[9]. Hybridization of elastin genomic probe pELN5-4, which spans elastin exons 31–33 and part of 36 (the human elastin gene has no exon 34 or 35), to *Pst*I digests of DNA from WS patient II-1 revealed a restriction fragment of 3.5 kb (allele 1) but not the common 2.0 and 1.5 kb fragments (allele 2). WS patient III-1 did not inherit the 3.5 kb *Pst*I fragment from his father; he only inherited the 2.0 and 1.5 kb fragments from his mother. The 3.3, 1.3, and 1.2 kb fragments are constant bands. *b*, Southern analysis[16] using *D2S44* which detects a VNTR polymorphism on chromosome 2 (ref. 24) and three additional VNTR markers (*D10S28* (ref. 25), *D14S13* (ref. 26) and *D17S26* (ref. 27); data not shown) showed the expected codominant inheritance in this kindred. These data indicate that affected father and son both carry a DNA deletion at the elastin locus and suggest that this mutation causes WS in this family. *c*, Pedigree structure and genotypes for kindreds with familial WS. Phenotypic designation was completed using standard criteria[28]. Individuals with the characteristic features of WS are indicated by filled circles (females) or squares (males). Empty circles or squares indicate unaffected individuals. In kindreds 1806 and 2042 the Williams phenotype is transmitted from parent to child. It was not possible genotypically to determine whether individual II-1 from K1806 and individual I-1 from K2042 were homozygous or hemizygous at the elastin locus. However, quantitative Southern analysis of DNA from these two individuals indicated dosage of 1:2 when compared with unaffected individuals, suggesting a hemizygosity at the elastin locus (data not shown). Genotypes for polymorphic markers at the elastin and adjacent loci are shown. Informed consent was obtained from each family member after the nature and possible consequences of the studies were explained.

inheritance greater than 99%, data not shown).

One elastin allele is deleted in WS

To determine if the WS-associated hemizygosity involved all, or only part, of the elastin gene, a contiguous set of cosmid and phage clones spanning the elastin gene was generated. Two cosmids at either end of the gene (cELN-272 and cELN-11D; Fig. 2) were used in Southern analyses to examine elastin gene dosage in DNA from patients and controls. Phosphorimage analyses of fragments detected by these elastin cosmids indicated dosage of about 2:1 when unaffected individuals were compared to WS subjects (Fig. 5, left and data not shown). DNA sample concentration was controlled by normalizing phosphorimage intensity to a band detected by a plasmid on chromosome 12. (Fig. 5, right and data not shown). These data suggest that the entire elastin locus is deleted in these WS patients.

Inherited and *de novo* deletions of the elastin locus were confirmed using fluorescent *in situ* hybridization (FISH). Elastin cosmids cELN-272 (Fig. 6) and cELN-11D (data not shown) hybridized to only one chromosome 7 homologue in all metaphase cells identified (50/50) from affected individuals II-1 of kindred 1806 (familial WS, Fig. 6*a*) and II-1 of kindred 1888 (sporadic WS, Fig. 6*b*). In unaffected controls, by contrast, both chromosome 7 homologues showed strong hybridization signals with the elastin probes (Fig. 6*c* and *d*). As a control, a second chromosome 7q-specific cosmid at 7q36 hybridized with both chromosome 7 homologues in metaphase cells from affected and unaffected individuals (Fig. 6). Identical findings were observed in FISH analyses of metaphase chromosomes from the other WS kindreds in this study (data not shown).

Size of WS-associated deletions

These WS-associated deletions were not visible by high-resolution cytogenetic analyses (data not shown). To determine if the deletion breakpoints were near the elastin gene, cosmids cELN-272 and cELN-11D which flank the elastin gene (Fig. 2) were used to screen for anomalous restriction fragments on pulsed field and agarose gels. No *Bam*HI, *Hind*III, *Sac*I, *Taq*I or *Not*I restriction fragment anomalies were identified (data not shown), consistent with the hypothesis that these deletions extended beyond the elastin gene and suggesting that the deletion breakpoints were outside the 114 kb defined by these cosmids.

Discussion

We conclude that WS can be caused by submicroscopic deletions within chromosomal subunit 7q11.23. Hemizygosity at the elastin locus was identified in every affected individual studied (9/9), suggesting that elastin hemizygosity is involved in the pathogenesis of this disease. Quantitative Southern analyses and FISH confirmed these findings and indicated complete deletion of one elastin allele in both familial and *de novo* WS. Together, these data suggest that deletion of one elastin allele is the mechanism of vascular and connective tissue pathology in WS.

Several further lines of evidence support a role for elastin in WS. First, the vascular pathology of WS, which is identical to that seen in autosomal dominant SVAS, shows abnormalities in elastic fibre architecture[11,12]; these pathologic findings could be caused by reduced or abnormal elastin. Second, the importance of elastic fibres for vascular structure and function suggests that reduced elastin would cause vascular disease. Third, we identified linkage between SVAS and the elastin gene in two families[7] and demonstrated disruption of the elastin gene in a third, suggesting that abnormalities in elastin can cause SVAS[8]. Finally, hemizygosity of the elastin gene could account for

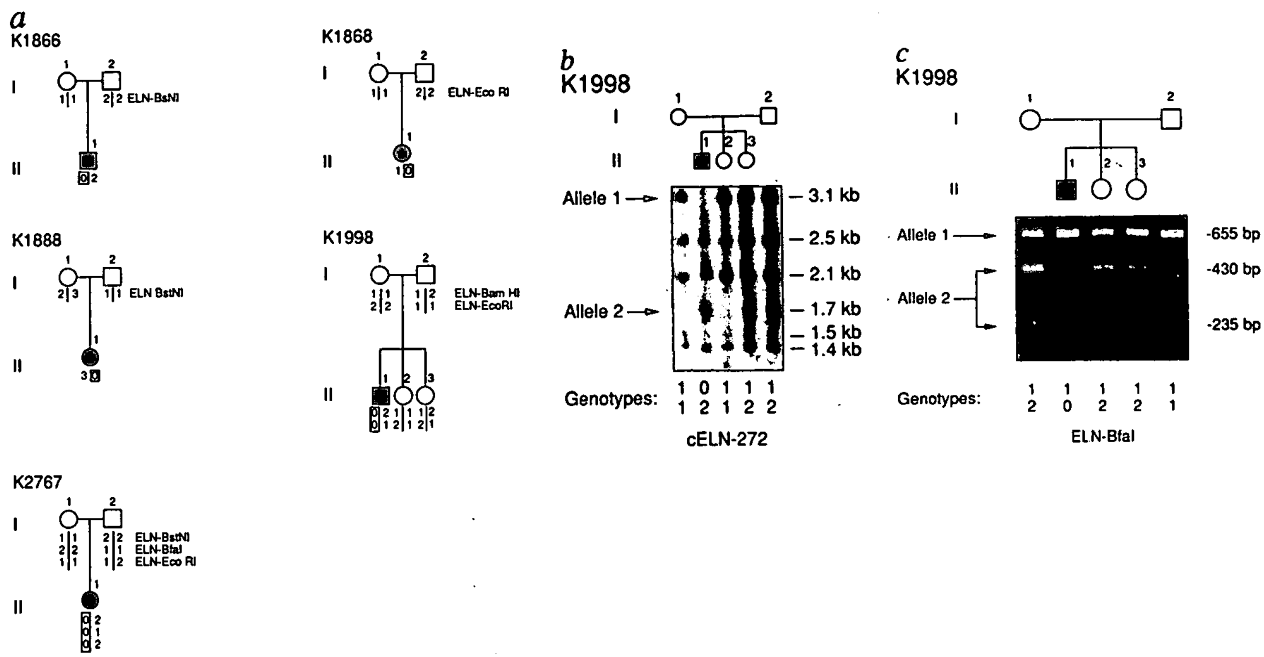

Fig. 4 Hemizygosity at the elastin locus in sporadic WS. *a*, Individuals from kindreds 1866, 1868, 1888, 1998 and 2767 represent sporadic cases of WS. Genotype analyses indicate hemizygosity at the elastin locus in all familial and sporadic WS cases. Informed consent was obtained from each family member after the nature and possible consequences of the studies were explained. *b*, Pedigree structure for kindred 1998, including a sporadic case of WS, is shown. Criteria for phenotypic classification were previously described[27]. Hybridization of elastin cosmid cELN-272 to *Bam*HI digests of DNA from this kindred showed that affected child II-1 failed to inherit a 3.1 kb allele (allele 1) from his mother. *c*, Genotypic analysis using elastin PCR polymorphism ELN-*Bfa*I[10] showed that the mother (individual I-1) was heterozygous at the elastin locus. These data indicate loss of heterozygosity at the elastin locus in this *de novo* case of WS.

all connective tissue abnormalities seen in WS, including hernias, premature aging of skin, joint laxity early in life followed by joint contractures, hoarse voice, diverticulosis of the bladder and colon, and dysmorphic facial features (loose connective tissue around the eyes, full cheeks, prominent lips and dental malocclusion)[2].

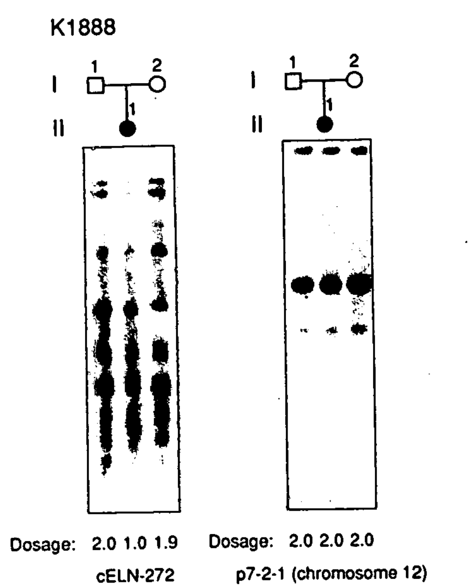

Fig. 5 Reduced dosage of the elastin gene in WS. Cosmids cELN-272 (left) and cELN-11D (not shown) which span the elastin gene were radiolabeled and hybridized with *Taq*I digests of DNA from kindred 1888. Phosphorimage analyses indicated dosage of about 2:1 when controls were compared to individual II-1 with WS. By contrast, when plasmid probe p7-2-1 (right), which spans the KCNA5 potassium channel gene on chromosome 12 (ref. 17), was hybridized with the same Southern filter, dosage was comparable for all family members, including individual II-1.

It is not yet clear why the connective tissue abnormalities of WS are more prominent than those found in autosomal dominant SVAS. Additional connective tissue abnormalities have been identified in some SVAS patients (hernias, mild dysmorphic facial features, fifth finger clinodactyly, hoarse voice[8,13]), but SVAS is primarily a vascular disease. The only SVAS mutation defined to date involves the 3' end of the elastin gene[8], whereas all WS-associated deletions described in this study involve the entire gene. The specific elastin mutation, therefore, may be responsible for some of the phenotypic differences between SVAS and WS. Alternatively, deleted loci adjacent to the elastin gene may modify the effects of elastin mutations.

The neurobehavioural features of WS are not easily explained by hemizygosity at the elastin locus, and our data suggest an alternative mechanism. Although occasional SVAS patients have dysmorphic facial features and other connective tissue abnormalities, none of the neurobehavioural features of WS have been documented in autosomal dominant SVAS. The mechanism of SVAS is incompletely defined, but probably involves reduced or abnormal elastin during development. Complete deletion of the elastin locus has not been identified in any SVAS family thus far (unpublished observations), suggesting that the mechanism may involve subtler mutations. The linkage and physical mapping data presented here indicate that WS-associated deletions extend beyond the elastin locus, spanning at least 114 kb. Additional genes, therefore, are probably deleted and one or more of the genes could be involved in the pathogenesis of this disease. It is possible, for example, that the severity of mental retardation in WS

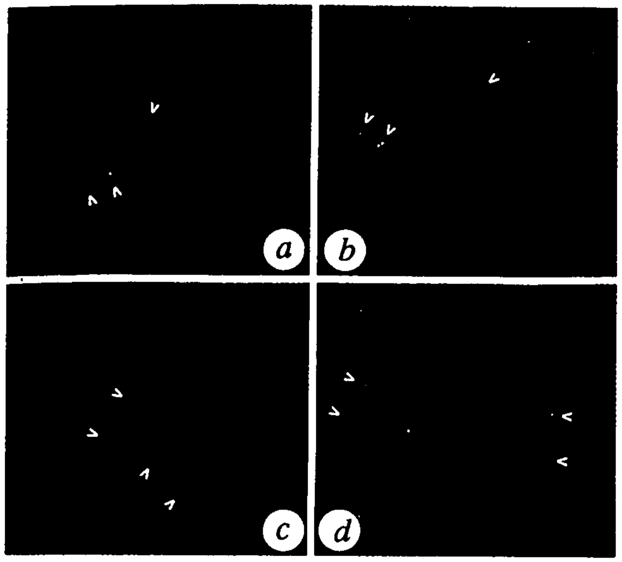

Fig. 6 Cytogenetic analysis of deletions involving the elastin locus in WS documented by fluorescent *in situ* hybridization (FISH). Elastin cosmid cELN-272 was hybridized with metaphase chromosomes from WS patients and unrelated controls. An additional chromosome 7-specific cosmid at locus *D7S396* (7q36) was cohybridized with elastin. WS patients K1806 individual II-1 (*a*) and K1888 individual II-1 (*b*) show hybridization signals (arrows) for the elastin cosmid on one chromosome 7 homologue but not the other. This finding was observed in 50/50 independent metaphase spreads for each patient. WS patients show signals on both chromosome 7 homologues with the 7q36-specific cosmid. *c,d,* In contrast, both chromosome 7 homologues in unaffected individuals show strong elastin hybridization and 7q36-specific cosmid signals. Photographs were taken directly from the photomicroscope and are unenhanced.

is related to the size of the deletion, a mechanism that could involve several genes. Refined linkage and physical mapping of chromosomal subunit 7q11.23, identification of genes adjacent to the elastin locus, and continued deletional analyses will determine if WS is a contiguous gene disorder.

It seems likely that submicroscopic deletions of the elastin gene will prove a common cause of WS. The ability to define deletions by FISH or genotype analysis will make presymptomatic diagnosis of this disorder feasible. Genetic testing of WS will also be a more accurate diagnostic tool for existing cases and will redefine phenotypic criteria for the disorder. The ability to predict and confirm WS will have immediate implications for management of this complex connective tissue and neurobehavioural disorder.

Methodology

Genomic library construction and screening. Cosmid libraries were constructed in pWEX15 (ref. 14). Cosmid vector pWEX15 was digested with *Xho*I and partially filled in with dCTP and dTTP using Klenow DNA polymerase, leaving 5'TC3' at the 5' end. Genomic DNA was partially digested with *Mbo*I and fractionated by sucrose-density gradient centrifugation to yield fragments of 35–42 kb. This DNA was partially filled in with dATP and dGTP using Klenow leaving 5'GA3' at the 5' end. Ligation was performed using 1 µg of vector and 2 µg of genomic DNA in a mixture containing 50 mM Tris-HCl, pH 7.8; 10 mM $MgCl_2$, 10 mM dithiothreitol, and 1 mM ATP. The reaction mixture was incubated with 2.5 U T4 DNA ligase (BRL) at 16 °C overnight and packaged with *in vitro* packaging extracts (Gigapack II-XL, Stratagene). About 2×10^5 cosmid clones were plated at low density. Plates were lifted with 1.2 mm Biotrans filters (ICN pharmaceuticals)[15]. Prehybridization was carried out in aqueous solution consisting of 5 × SSPE, 5× Denhardt's solution, 0.5% SDS, and 500 µM ml^{-1} sheared human placental DNA for 4 h. ^{32}P-labelled probe DNA was added directly to prehybridization solution to $> 2 \times 10^6$ cpm ml^{-1}. Hybridization was performed overnight at 65 °C. Filter washes consisted of two 25 °C washes in 2× SSC, 0.1% SDS for 15 min each, two 25 °C washes in 0.1× SSC, 0.1% SDS for 15 min each, and a final 65 °C wash in 0.1X SSC, 0.1% SDS for 2 min. Filters were exposed for autoradiography on Kodak XAR-5 film at –70 °C with two intensifying screens (Lightening Plus, Dupont).

Received 4 June; accepted 28 June 1993.

Southern analyses. DNA restriction enzyme digestions were carried out as recommended by the manufacturer (New England Biolabs) with the exception that 2- to 5-fold excess enzyme was used. 5 µg of digested DNA was separated on 1% agarose gels in 2 × Tris-acetate buffer and transferred to nylon membrane (Hybond-N^+, Amersham)[16]. Plasmids, cosmids, and subclones were radiolabelled and membranes hybridized as described[7].

PCR-based genotypic analyses. Polymorphic sequences at the *ELN* locus[10] were amplified by PCR as described[7]. Products were incubated with *Bst*NI or *Bfa*I, run on a 3.5% NuSieve/0.5% LE agarose gel, and stained with ethidium bromide.

Phosphorimage analysis. Phosphorimage analysis was carried out on a Molecular Dynamics Imager (Sunnyvale, CA). Samples were normalized by comparing to dosage values with a chromosome 12 plasmid p7-2-1 (ref. 17).

Florescence *in situ* hybridization (FISH). *In situ* hybridization was carried out using EBV-transformed lymphoblastoid cell lines[18]. Metaphase chromosomes from lymphoblastoid cell lines and normal peripheral blood were prepared and G-banded as described[19]. Following photography of G-banded chromosomes and before *in situ* hybridization, slides were destained using published techniques[20]. For *in situ* hybridization cosmids cELN-11D, cELN-272 and cMKA1 (a marker for chromosome 7, 7q35-qter) were labelled with biotin-14-dATP (BRL) and FITC-12-dUTP (Boehringer Mannheim) using a nick translation kit (BRL). Prehybridization, hybridization and detection procedures described[21,22] were used with the following modifications. Cosmids cELN-11D or cELN-272 (10 ng µl^{-1}), herring testes DNA (1 µg µl^{-1}), human placental DNA (250 ng µl^{-1}), with or without chromosome 7 marker cMKA1 (10 µg µl^{-1}) were denatured together and allowed to preanneal for 3 h at 37 °C in a hybridization mix of 50% formamide, 10% dextran sulfate and 2× SSC. The slides were denatured at 72 °C for 2 min. Following overnight hybridization at 37 °C, slides were washed in 50% formamide, 2× SSC at 43 °C for 15 min and 2× SSC at 37 °C for 8 min. For detection of hybridization, slides were incubated in blocker 1 (Oncor) for 5 min at room temperature, then incubated with ExtrAvidin-FITC (10 mg ml^{-1}) (Sigma) for 20 min at 37 °C. Slides were then washed with PBD buffer (Oncor) for 6 min at room temperature, incubated with blocker 2 (Oncor) for 5 min at room temperature, incubated with anti-avidin (Oncor) for 20 min at 37 °C, followed by PBD, blocker 1 and ExtrAvidin incubation. Following the amplification step, the slides were washed with PBD and chromosomes counterstained with a DABCO (Sigma) and propidium iodide (0.5 mg ml^{-1}, Sigma) mix. Metaphases were photographed using a Zeiss Axioscope, equipped for epifluorescence, and photographed with Kodak Ektachrome 100 HC.

Acknowledgements
We thank M. Curran, R. White, L. Ptacek, S. Odelberg and L. Veasy for advice and suggestions; H. Rienhoff, D. Viskochil, C. Leonard, L. Bartlett and J. Carey for critical review of the manuscript; and B. Otterund, T. Varvil, M. Woodward, S. Austin and S. Nelson for technical support. This work was supported by NIH grant RO1HL4807, the Williams Syndrome Foundation, the American Heart Association, Public Health Service Research Grant MO1-RR00064 from the National Center for Research Resources, a Syntex Award, a March of Dimes Grant, and the Technology Access Section of the Utah Genome Center.

1. Beuren, A.J. Supravalvular aortic stenosis: a complex syndrome with and without mental retardation. *Birth Defects* 8, 45–46 (1972).
2. Morris, C.A., Demsey, S.A., Leonard, C.O., Dilts, C. & Blackburn, B.L. Natural history of Williams syndrome. *J. Pediatr.* 113, 318–326 (1988).
3. Bellugi, U., Bihrle, A., Jernigan, T., Trauner, D. & Doherty, S. Neurophysical, neurological, and neuroanatomical profile of Williams syndrome. *Am. J. med. Genet.* 6, 115–125 (1990).
4. Dilts, C., Morris, C, & Leonard, C. Hypothesis for development of a behavioral phenotype in Williams syndrome. *Am. J. med. Genet.* 6, 126–131 (1990).
5. Chevers, N. Observations on the diseases of the orifice and valves of the aorta. *Guys Hosp. Rep.* 7, 387–421 (1842).
6. Eisenberg, R., Young,D., Jacobson, B. & Voito, A. Familial supravalvular aortic stenosis. *Am J. Dis. Child.* 108, 341–347 (1964).
7. Ewart, A.K. *et al.* A human vascular disorder, supravalvular aortic stenosis, maps to chromosome 7. *Proc. natn. Acad. Sci. U.S.A.* 90, 3226–3230 (1993).
8. Curran, M.E. *et al.* The elastin gene is disrupted by a translocation associated with supravalvular aortic stenosis. *Cell* 73, 159–168 (1993).
9. Morris,C., Thomas, I.T. & Greenberg, F. Williams syndrome: autosomal dominant inheritance. *Am. J. med. Genet.* (in the press).
10. Tromp, G. *et al.* A to G polymorphism in *ELN* gene. *Nucl. Acids Res.* 19, 4314 (1991).
11. Perou, M. Congenital supravalvular aortic stenosis. *Arch. Pathol.* 71, 113–126 (1961).
12. O'Connor, W. *et al.* Supravalvular aortic stenosis: clinical and pathologic observations in six patients. *Arch. Pathol. Lab. Med.* 109, 179–185 (1985).
13. Morris,C.A., Loker, J., Ensing, G. & Stock, A.D. Supravalvular aortic stenosis cosegregates with a familial 6;7 translocation which disrupts the elastin gene. *Am. J. med. Genet.* 46, 737–744 (1993).
14. Wahl, G.M. *et al.* Cosmid vectors for rapid genomic walking, restriction mapping, and gene transfer. *Proc. natn. Acad. Sci. U.S.A.* 84, 2160–2164 (1987).
15. Benton, W.D. & Davis, R.W. Screening l-gt recombinant clones by hybridization to single plaques *in situ*. *Science* 196, 180–182 (1977).
16. Southern, E.M. Detection of specific sequences among DNA fragments separated by gel electrophoresis. *J. molec. Biol.* 98, 503–517 (1975).
17. Curran, M.E. Landes, G.M. & Keating, M.T. Molecular cloning, characterization and genomic organization of a human cardiac potassium channel gene. *Genomics* 12, 729–737 (1992).
18. Kunkel, L.M. *et al.* Analysis of human Y-chromosome-specific reiterated DNA in chromosome variants. *Proc. natn. Acad. Sci. U.S.A.* 74, 1245–1249 (1977).
19. Goodman, B.K., Xu, W., Nottoli, V., Rundall-Jackson, T. & Stock, A.D. A simple technique for bone marrow preparations with modified hypotonic treatment. *Karyogram* 11, 95–96 (1985).
20. Klever, M., Grond-Ginsbach, C., Scherthan, H. & Schroeder-Kurth, T.M. Chromosomal *in situ* hybridization after giemsa banding. *Hum. Genet.* 86, 484–486 (1991).
21. Pinkel, D. *et al.* Fluorescence *in situ* hybridization with human chromosome-specific libraries: detection of trisomy 21 and translocations of chromosome 4. *Proc. natn. Acad. Sci. U.S.A.* 85, 9138–9142 (1988).
22. Tkachuk, D. *et al.* Detection of *bcr-abl* fusion in chronic myelogeneous leukemia by *in situ* hybridization. *Science* 250, 559–562 (1990).
23. Fazio, M.J. *et al.* Human elastin gene: new evidence for localization of elastin to the long arm of chromosome 7. *Am. J. hum. Genet.* 48, 696–703 (1991).
24. O'Connell, P. *et al.* Twenty loci form a continuous linkage map of marker for human chromosome 2. *Genomics* 5, 738–745 (1989).
25. Vogelstein, B. *et al.* Allelotype of colorectal carcinomas. *Science* 244, 207–211 (1989).
26. Nakamura, Y. *et al.* Variable number of tandem repeat markers for human gene mapping. *Science* 235, 1616–1622 (1987).
27. Nakamura, Y. *et al.* A mapped set of DNA markers for human chromosome 17. *Genomics* 2, 302–309 (1988).
28. Preus, M. The Williams syndrome: Objective definition and diagnosis. *Clin. Genet.* 24, 433–438 (1984).

STIC-ILL

QH431. A1 H86

~~NPL~~

From: Chen, Shin-Lin
Sent: Wednesday, January 15, 2003 6:10 PM
To: STIC-ILL
Subject: articles

Please provide the following articles ASAP. thanks!
Serial No. 09/258,217.

L4 ANSWER 28 OF 85 CAPLUS COPYRIGHT 2003 ACS
AU Olson, Timothy M.; Michels, Virginia V.; Urban, Zsolt; Csiszar, Katalin; Christiano, Angela M.; Driscoll, David J.; Feldt, Robert H.; Boyd, Charles D.; Thibodeau, Stephen N.
TI A 30 kb deletion within the elastin gene results in familial supravalvular aortic stenosis
SO Human Molecular Genetics (1995), 4(9), 1677-9
CODEN: HMGEE5; ISSN: 0964-6906

L4 ANSWER 29 OF 85 CAPLUS COPYRIGHT 2003 ACS
AU Mari, A; Amati, F.; Mingarelli, R.; Giannotti, A.; Sebastio, G.; Colloridi, V.; Novelli, G.; Dallapiccola, B.
TI Analysis of the elastin gene in 60 patients with clinical diagnosis of Williams syndrome
SO Human Genetics (1995), 96(4), 444-8.

L4 ANSWER 20 OF 85 CAPLUS COPYRIGHT 2003 ACS
AU Lindahl, Per; Karlsson, Linda; Hellstrom, Mats; Gebre-Medhin, Samuel; Willetts, Karen; Heath, John K.; Betsholtz, Christer
TI Alveogenesis failure in PDGF-A-deficient mice is coupled to lack of distal spreading of alveolar smooth muscle cell progenitors during lung development
SO Development (Cambridge, United Kingdom) (1997), 124(20), 3943-3953.

L4 ANSWER 40 OF 85 CAPLUS COPYRIGHT 2003 ACS
AU Ewart, Amanda K.; Morris, Colleen A.; Atkinson, Donald; Jin, Weishan; Sternes, Keith; Spallone, Patricia; Stock, A. Dean; Leppert, Mark; Keating, Mark T.
TI Hemizygosity at the elastin locus in a developmental disorder, Williams syndrome
SO Nature Genetics (1993), 5(1), 11-16.

L4 ANSWER 31 OF 85 CAPLUS COPYRIGHT 2003 ACS
AU Dallapiccola, B.; Amati, F.; Gennarelli, M.; Mari, A.; Novelli, G.
TI Advances in molecular analysis of congenital heart defects
SO Bulletin of Molecular Biology and Medicine (1995), 20(3,4), 135-140.

Shin-Lin Chen
AU 1632
CM1 12A15
Mail Box: CM1 12E12
(703) 305-1678

Hum Genet (1995) 96:444–448

ORIGINAL INVESTIGATION

A. Mari · F. Amati · R. Mingarelli · A. Giannotti
G. Sebastio · V. Colloridi · G. Novelli · B. Dallapiccola

Analysis of the elastin gene in 60 patients with clinical diagnosis of Williams syndrome

Received: 30 October 1994 / Revised: 23 December 1994

Abstract Williams syndrome (WS) is caused by deletion of the elastin (ELN) gene. We have analyzed an intragenic restriction fragment length polymorphism (RFLP) and the gene dosage of ELN using a new probe (FP4) in a series of 60 sporadic patients with a clinical diagnosis of WS. Deletion of the ELN gene was shown in 54 cases, while clinical revaluation of the 6 patients without the deletion did not confirm the diagnosis of WS. These results support the genetic homogeneity of WS, and the high accuracy of ELN molecular analysis, which can be confidenty used for providing genetic counselling to WS families.

Introduction

Williams syndrome (WS; MIM* 194050) is a developmental disorder characterized by mental and statural deficiency, elfin face, supravalvular aortic stenosis (SVAS) and peripheral pulmonary arterial stenoses, and infantile hypercalcemia (Beuren 1972; Morris et al. 1988). WS usually occurs sporadically, although it can be inherited as an autosomal dominant disorder (Morris et al. 1993; Sadler et al. 1993). Based on ascertainment of severe cases, Grimm and Wesselhoeft (1980) have estimated the frequency of WS as 1 in 10,000. Hemizygosity at the elastin (ELN) locus was identified in patients with WS, demonstrating that inherited and de novo ELN deletions are responsible for the pathogenesis of this disorder (Ewart et al. 1993). An ELN defect could explain the vascular abnormalities observed in WS, which are similar to those found in the autosomally dominant SVAS, in which linkage and molecular studies have proved a causal relationship with ELN gene mutations (Curran et al. 1993). Therefore, both WS and SVAS appear to be caused by submicroscopic deletions of 7q11.23.

We report the molecular study of 60 sporadic patients with clinical diagnosis of WS evaluated using an intragenic polymorphism and DNA gene dosage analysis of the ELN locus, which corroborates the relationship between this disease and ELN gene deletions.

Materials and methods

Clinical ascertainment

Sixty patients with a clinical diagnosis of WS (Morris et al. 1988) were referred for molecular analysis by three Paediatric and Cardiological Units in a 10-month period. The patients age at diagnosis ranged from 7 months to 22 years. Fifty-four patients had classic WS. On the basis of the Preus diagnostic index (Preus 1984), all these patients showed a total score higher than 4 (5.37 ± 1.22). Mental retardation and facial dysmorphisms were present in all cases. Additional features were hoarse voice in 45 patients (83%), failure to thrive and strabismus in 25 (46%), microbrachycephaly in 22 (40%), stellate iris in 35 (64%), SVAS in 44 (81%), other congenital heart disease in 12 (22%), hypertension in 2, constipation in 17 (31%), inguinal hernias in 42 (23%), joint laxity in 28 (50%), ciphosis in 16 (29%), and lordosis in 14 (26%). No patient had hypercalcemia. Six patients were considered "atypical", with mental retardation and facial features reminiscent of WS as prominent characteristics. In these patients the Preus index was invariably negative (– 2.74 ± 1.40).

Standard and high resolution chromosome analysis was normal in all patients.

Polymerase chain reaction (PCR)-based genotyping and DNA dosage analysis

DNA was isolated from peripheral blood collected in EDTA (Novelli et al. 1987). ELN hemizygosity was determined in 53 nuclear

A. Mari · F. Amati · R. Mingarelli · B. Dallapiccola (✉)
Cattedra di Genetica Umana, Università Tor Vergata,
Via di Tor Vergata 135, I-00133 Roma, Italy

R. Mingarelli · B. Dallapiccola
Servizio di Genetica Medica, Ospedale CSS, IRCCS,
San Giovanni Rotondo, Italy

A. Giannotti
Servizio di Genetica Medica,
Ospedale Pediatrico Bambino Gesù, Roma, Italy

G. Sebastio
Dipartimento di Pediatria, Università Federico II, Napoli, Italy

V. Colloridi
Clinica Pediàtrica, Università La Sapienza, Roma, Italy

G. Novelli
Cattedra di Genetica Umana,
Università Cattolica del Sacro Cuore, Roma, Italy

Fig. 1 A Complete nucleotide sequence of FP4 probe. Oligonucleotide primer sequences used to amplify the fragment are *boxed with arrow*. *Bst*NI sites are *underlined*. Exons are delimited by *filled arrowheads*. B Schematic representation of allele generated by *Bst*NI digestion

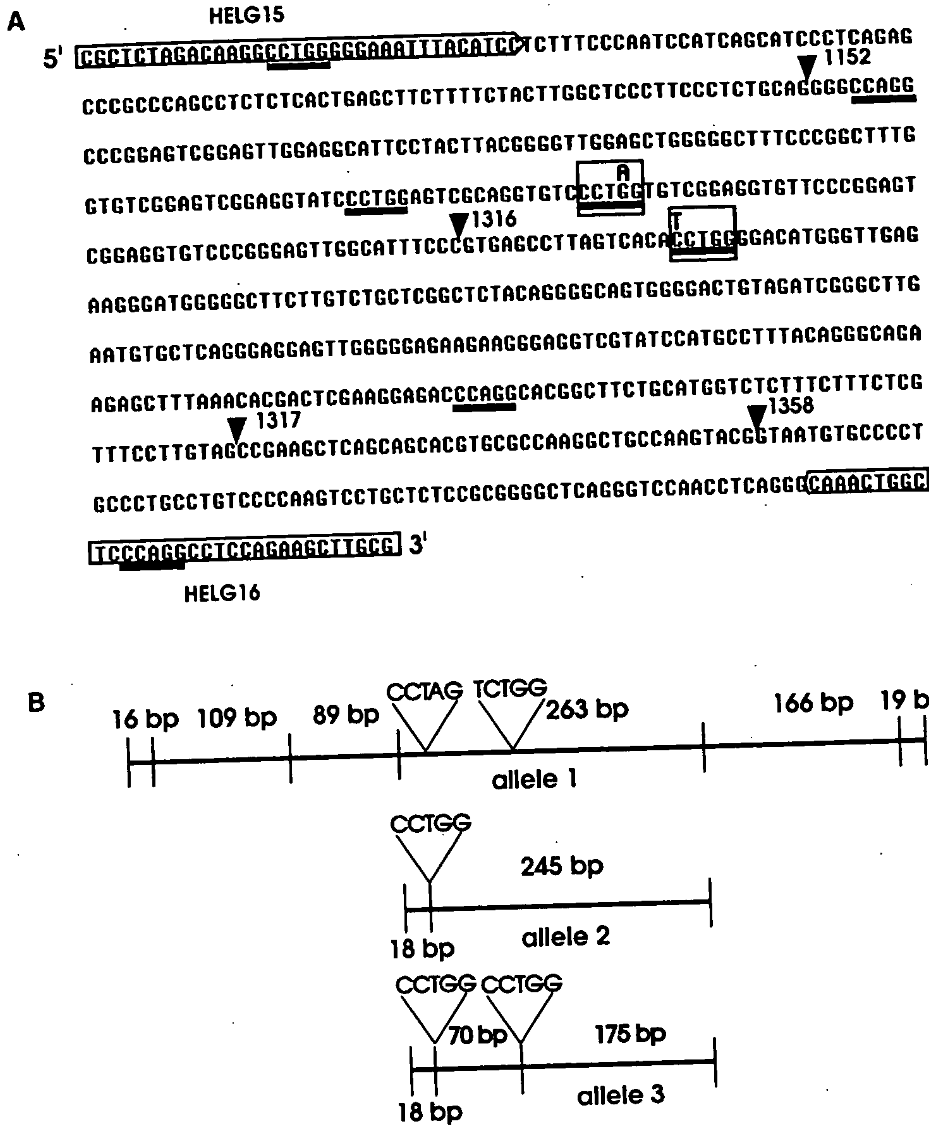

families by genotype analysis of an intragenic *Bst*NI/422A→G polymorphism (Tromp et al. 1992). Misinheritance was excluded by paternity testing using three DNA polymorphisms (D1S80, APOB, HLADQα) (Novelli et al. 1992).

DNA dosage analysis was determined by Southern blotting in all patients. DNA samples (10 μg) were digested with *Hin*dIII according to the manufacturer's recommendations, fractionated by electrophoresis through 0.8% agarose gels, and transferred to Hybond N membranes (Amersham). Blots were probed simultaneously with pFP4 and pTNT800 (Samson et al. 1990) as control probe. FP4 is the PCR product generated by HELG15 and HELG16 oligonucleotide primers (Tromp et al. 1992). This 660-bp genomic fragment, which contains exons 15 and 16 and flanking intron sequences (Fazio et al. 1988), was directly ligated with pCR II using the TA Cloning System (Invitrogen Corp., USA), according to the manufacturer's recommendations. The ligation mixture were transformed into competent DH5′αF⁻ *Escherichia coli* cells (Clontech, USA), and positive clones were identified as white colonies after plating in LB agar containing ampicillin (50 μg/ml 5-bromo-4-chloro-3-indolyl-β-D-galactophyranoside and (X-Gal 45 mg/ml). Recombinant plasmids were purified and digested with *Eco*RI to determine the size of inserts. Approximately 50 ng of pure DNA plasmid was used for cycle sequencing (CircumVent Kit, Biolabs, USA). Plasmid DNA was combined in a 0.5 ml microcentrifuge tube containing 2 pmol of the M13 forward (-38) or M13 reverse primer labeled with the infrared dye IRD40 (LI-COR, USA), 1 × CircumVent sequencing buffer, 1 U of Vent(exo-)DNA polymerase (Biolabs, USA), 1 μl of 30 × Triton X-100, and sterile water to 14 μl of final volume. Then 3.2 μl of this mixture was added to appropriate tubes containing dideoxynucleotide triphosphates and subjected to 25 repetitive cycles of denaturation, annealing, and chain extension at 95°C, 60°C and 72°C, respectively, for 20 s. Aliquots of 2 μl were denatured by heating and loaded onto a denaturing polyacrylamide gel. The nucleotide sequence was established using a LI-COR Model 4000 automated DNA sequencer (Fig. 1). Purified FP4 inserts and the pTNT800 control probe were labeled to a specific activity of 0.3×10^{-9}–1.0×10^{-9} Cerenkov cpm/μg DNA, according to Feinberg and Vogelstein (1983). Following hybridization, membranes were rinsed twice in 2 × SSC at room temperature and washed 30 min each in 2 × SSC and 1 × SSC, 0.1% sodium dodecyl sulfate (SDS), respectively at 65°C. Hybridization signals were quantitated by densitometry using a Molecular Dynamics ImageQuant software (Molecular Dynamics, USA). Hemizygosity was defined as a signal strength ratio of < 0.5, whereas ratios of ≥ 0.9 were taken as indicating a normal copy number. Each sample was examined three times and the mean of the determinations was taken as final value.

Results

Restriction fragment length polymorphism (RFLP) analysis

Fifty-three of the 60 patients, including 51 with classical WS and 2 atypical cases, for which parental DNA was also available, were evaluated by RFLP analysis using the intragenic PCR-based *Bst*NI/422G→A polymorphism. This biallelic polymorphism was originally described by Tromp et al. (1992). Restriction analysis of the amplified region from several individuals has shown the presence of a third allele generated by a C/T transition that creates a *Bst*NI site 70 bp downstream of the originally reported *Bst*NI site (Fig. 1). Therefore, this RFLP system detects three alleles at this locus of 262, 244 and 175 bp, respectively, with a frequency of 0.40, 0.44 and 0.16 in the Italian population (Fig. 2). The genotype frequencies are in fitting with the Hardy-Weinberg equilibrium in a sample of 100 unrelated Caucasian individuals (adult donors to the National Blood Transfusion Center, Italian Red Cross, Rome). Only 17 (32%) families were informative. De novo ELN allele loss was found in 15 patients with classic WS, while no evidence for hemizygosity was obtained in the 2 atypical informative cases. The deletion occurred in the paternal chromosome in 8 patients and in the maternal chromosomes in the remaining 9 excluding any preferential parental inheritance.

The 60 WS patients, including those for which parental DNA was not available or RFLP was not informative, were analyzed by dosage analysis. Figure 3 shows a representative autoradiogram of a Southern blot of two patients and two controls. The blot was cohybridized with the FP4 test probe and the TNT800 control probe, in order to determine the copy number at the ELN locus. Visual inspection showed that the intensity of the 12 kb band recognized by FP4 was markedly reduced compared with the control probe in all patients with classic WS, but not in normal subjects. Quantitation of the hybridization signals confirmed that the 54 patients with classic WS had one copy only of the ELN gene (Fig. 3). The 6 patients with atypical WS had a normal gene copy number (intensity values > 0.9 on three occasions). These patients were also re-evaluated using the diagnostic index developed by Preus (1984), which showed total score values in the range of non-WS patients.

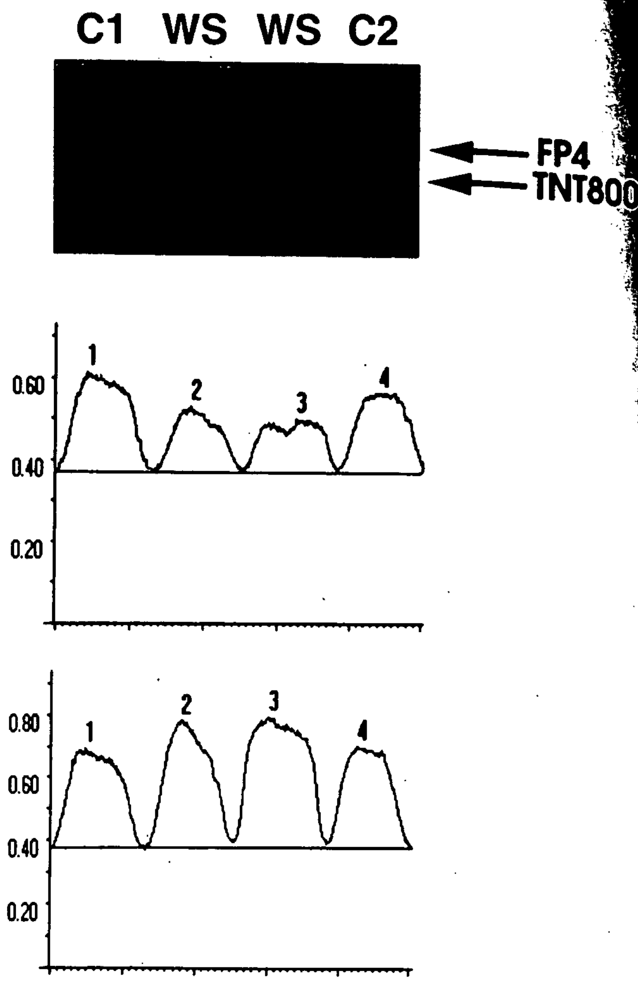

Fig. 3 Hemizygosity at the ELN locus detected by FP4 probe analysis and densitometric signal quantification

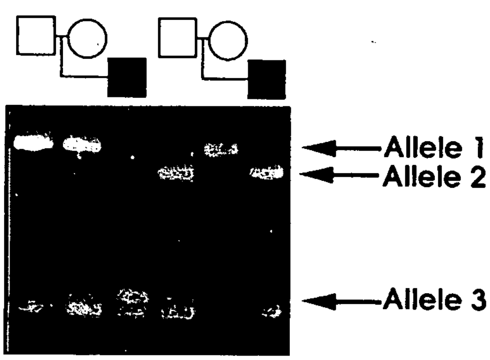

Fig. 2 Polymerase chain reaction (PCR) genotyping at ELN locus using HELG15 and HELG16 oligonucleotide primers in two nuclear WS families

Discussion

ELN deletions were first detected in a series of five sporadic and four familial WS patients, examined for the ELN gene. Hemizygosity at this locus was demonstrated in each of the affected patients suggesting that ELN hemizygosity is pathogenetically related to this disease (Ewart et al. 1993). In a series of subsequent studies, ELN deletion was demonstrated in 203 of 209 patients with classic WS, using intragenic polymorphisms, DNA dosage analysis or fluorescent in situ hybridization (FISH) (Greenberg et al. 1994; Morris et al. 1994; Morimoto et al. 1994; Robinson et al. 1994; Smoot et al. 1994). Our results on 54 additional patients with classic WS corroborate previous evidence, by showing that the ELN deletion occurs in all patients excluding genetic heterogeneity. In fact, clinical re-examination of the six patients not carrying the

deletion did not confirm the diagnosis of WS. However, three patients without the deletion in the series of Morris et al. (1994) and two patients in the series of Greenberg et al. (1994), were considered affected by classical WS, while one such patient in the series of Greenberg et al. (1994) was considered to have atypical WS. The proposed explanation for these observations is that the patients had a small deletion not detected by the utilized probes. This idea is also in keeping with the observation of a mildly affected WS patient in the SVAS family in which a "balanced" t(6;7) had disrupted the ELN gene within exon 28 (Morris et al. 1993). Furthermore, three studies at least, including ours, have performed ELN gene analysis in heterogeneously selected patients including cases with uncertain diagnosis. A total of 74 patients have been investigated, 16 of which have proved to be affected by WS as shown by ELN gene deletion (Morris et al. 1994; Lowery et al. 1994). The comprensive results of molecular analysis support the idea that the ELN deletion is pathogenetically related to classic WS in not less than 97% to 98% of patients (257/263). It is likely that those cases in which deletion was not detected have a small ELN deletion overlooked by the probes used. In addition, analysis of patients with an atypical WS phenotype also proves that molecular analysis is useful in detecting atypical or less typical WS patients. This analysis also proves to be useful in evaluating patients in the first year of life, when WS diagnosis can be more problematic, and in testing familial transmission of this disorder.

Haploinsufficiency of ELN provides a biological basis for the abnormal elastic fiber properties seen in WS patients, including vascular pathology, hernias, premature aging of skin, joint laxity and contractures, hoarse voice, bladder and colon diverticulosis, and dysmorphic facial characteristics (Preus 1984; Greenberg 1990; Ardinger et al. 1994). In fact, the reduced synthesis of tropoelastin could well alter fiber assembly and cause generalized connective tissue abnormalities. Partial deletions of ELN has been shown in SVAS patients in which only those elastic tissues exposed to extreme mechanical stress, like the aortic root, express this molecular defect at the clinical level (Dietz and Pyeritz 1994). Therefore, the phenotypic differences between WS and SVAS, could be a different dosage of tropoelastin. This hypothesis awaits support by identification of additional mutations associated with SVAS or the development of functional mutation tests. Nevertheless, the neurobehavioral features and the hypercalcemia of WS are not explained by a gene dosage effect of tropoelastin, although ELN is a housekeeping gene and is expected to be functional in all cell types (Rosenbloom 1993). It is also possible that other genes flanking ELN are deleted in WS (Ewart et al. 1993). Present results have shown that the ELN deletions found in WS patients span 114 kb of genomic DNA, whereas the ELN gene spans 45 kb of genomic DNA (Fazio et al. 1991; Ewart et al. 1993). The molecular events underlying ELN deletions in WS are not understood at present. Interestingly the calcitonin receptor (CTR) gene has been mapped to 7q21.11–21.13, 10 Mb telomeric to the ELN gene, located at 7q11.23 (Perez-Jurado et al. 1994). It is possible that a more complex rearrangement affecting this critical 7q region accounts for the 5%–10% of WS patients with infantile hypercalcemia.

The diagnosis of WS is currently based on careful clinical examination and is often hampered by the variability of the disease. Since some complications of WS, including obstruction of cardiac output, myocardial ischemia, impaired pulmonic flow and cerebrovascular accidents, are often life threatening, early diagnosis of the patients is extremely important. Genetic testing of WS using the protocol described in this study and/or FISH analysis (Ewart et al. 1993; Lovery et al. 1994) make presymptomatic diagnosis of this disorder feasible. Analysis of the triallelic ELN polymorphism described in the present study, is not per se informative enough to be used in routine diagnostic protocols. On the contrary, analysis using the FP4 probe, which is available for diagnostic use, appears highly accurate and informative. The application of this molecular protocol improves genetic counselling in WS families and probands, especially in the first year of life when the clinical diagnosis is more difficult and can be applied to clarify those cases in which parental segregation of a mildly expressed WS is suspected.

Acknowledgements This work was supported in part by ASM (Milan) and the Italian Ministry of Education and Health. FP4 probe is available on request.

References

Ardinger RH, Goertz KK, Mattioli LF (1994) Cerebrovascular stenoses with cerebral infarction in a child with William syndrome. Am J Med Genet 51 : 200–202

Beuren AJ (1972) Supravalvular aortic stenosis: a complex syndrome with and without mental retardation. Birth Defect VIII: 45–56

Curran ME, Atkinson DL, Ewart AK, Morris CA, Leppert M, Keating MT (1993) The elastin gene is disrupted by a translocation associated with supravalvular aortic stenosis. Cell 73: 159–168

Dietz HC, Pyeritz RE (1994) Molecular genetic approaches to the study of human cardiovascular disease. Annu Rev Physiol 56: 763–796

Ewart AK, Morris CA, Atkinson D, Jin W, Sternes K, Spallone P, Stock AD, Leppert M, Keating MT (1993) Hemizygosity at the elastin locus in a developmental disorder, Williams syndrome. Nature Genet 5 : 11–16

Fazio MJ, Olsen DR, Eunkyung A, Kauh BA, Clinton TB, Indik Z, Goldestein-Ornstein N, Yeh H, Rosenbloom J, Uitto G (1988) Cloning of full-length elastin cDNAs from a human skin fibroblast recombinant cDNA library: further elucidation of alternative splicing utilizing exon specific oligonucleotides. J Invest Dermatol 91 : 458–464

Fazio MJ, Mattei MG, Passarge E, Chu ML, Black D, Solomon E, Davidson JR, Uitto J (1991) Human elastin gene: new evidence for localization to the long arm of chromosome 7. Am J Hum Genet 48 : 696–703

Feinberg AP, Vogelstein B (1983) A technique for radiolabeling DNA restriction endonuclease fragments to high specific activity. Anal Biochem 132 : 6–11

Greenberg F (1990) Williams syndrome: professional symposium. Am J Med Genet 6 : 85–88

Greenberg F, Nickerson E, McCaskill C, Keating M, Shaffer LG (1994) Deletions of the elastin gene in Williams Syndrome. Am J Hum Genet 55 : [Suppl]A41(213)

Grimm T, Wesselhoeft H (1980) Zur Genetik des Williams-Beuren-Syndroms und der isolierten Form der supravalvulaeren Aorten-stenose (Untersuchungen von 128 Familien). Z Kardio 69: 168–172

Lowery M, Brothman L, Ewart A, Morris C, Keating M, Leonard C, Carey J, Brothman A (1994) Application of ELN cosmid probes using fluorescence in situ hybridization (FISH) toward a clinical diagnostic test for Williams syndrome. Am J Hum Genet 55: [Suppl]A38(194)

Morimoto Y, Kuwano A, Kuwajiama K, Fukushima Y, Ganaha H, Ashimine K, Tsukahara M, Kondo I (1994) Hemizygosity at the elastin locus and clinical features of Williams Syndrome. Am J Hum Genet 55: [Suppl]A362(2126)

Morris CA, Susan A, Demsey M, Leonard CO, Dilts C, Blackburn BL (1988) De natural history of Williams syndrome: physical characteristics. J Pediatr 113: 318–326

Morris CA, Thomas IT, Greenberg F (1993) Williams syndrome: autosomal dominant inheritance. Am J Med Genet 47: 478–481

Morris CA, Ewart AK, Sternes K, Spallone P, Stock AD, Leppert M, Keating MT (1994) Am J Hum Genet 55: [Suppl]A88(493)

Novelli G, Potenza L, Ruzzo A, Dallapiccola B (1987) Polymorphic DNA markers linked to cystic fibrosis locus in 20 Italian nuclear families. Gene Geogr 1: 193–199

Novelli G, Spinella A, Gennarelli M, Mingarelli R, Dallapiccola B (1992) Analysis of APOB, HLADQalpha, and D1S80 polymorphisms in the Italian population using the polymerase chain reaction. Am J Hum Biol 4: 381–386

Perez-Jurado LA, Peoples R, Kaplan P, Mariman ECM, Francke U (1994) Deletion and candidate genes in Williams syndrome. Am J Hum Genet 55: [Suppl]A42(214)

Preus M (1984) The Williams syndrome: objective definition and diagnosis. Clin Genet 25: 422–428

Robinson WP, Kotzot D, Bernasconi F, Schinzel AA (1994) Elastin deletion in Williams syndrome. 26th Annual Meeting, ESHG, Paris, France, June 1–5, 1994, A20

Rosembloom J (1993) Elastin. In: Royce PM, Steinmann B (eds) Connective tissue and its heritable disorders. Willey-Liss, New York, pp 167–188

Sadler LS, Robinson LK, Verdaasdonk KR, Gingell R (1993) The Williams syndrome: evidence for possible autosomal dominant inheritance. Am J Med Genet 47: 468–470

Samson F, Lee JE, Hung DW, Potter TG, Herbstreith M, Roses AD, Gilbert JR (1990) Isolation and localization of a slow troponin (TnT) gene on chromosome 19 by subtraction hybridization of a cDNA muscle library using myotonic dystrophy muscle cDNA. J Neurosci Res 27: 441–451

Smoot LB, Lacro RV, Pober B, Kunkel LM (1994) Molecular genetic analysis of individual with Williams syndrome and Supravalvar Aortic Stenosis. Am J Hum Genet 55: [Suppl]A243 (1420)

Tromp G, Christiano A, Goldstein N, Indik Z, Boyd C, Rosenbloom J, Deak S, Prockop D, Kuivaniemi H (1992) A to G polymorphism in ELN gene. Nucleic Acids Res 19: 4314

QL951.D48
NPL

From: Chen, Shin-Lin
Sent: Wednesday, January 15, 2003 6:10 PM
To: STIC-ILL
Subject: articles

Please provide the following articles ASAP. thanks!
Serial No. 09/258,217.

L4 ANSWER 28 OF 85 CAPLUS COPYRIGHT 2003 ACS
AU Olson, Timothy M.; Michels, Virginia V.; Urban, Zsolt; Csiszar, Katalin; Christiano, Angela M.; Driscoll, David J.; Feldt, Robert H.; Boyd, Charles D.; Thibodeau, Stephen N.
TI A 30 kb deletion within the elastin gene results in familial supravalvular aortic stenosis
SO Human Molecular Genetics (1995), 4(9), 1677-9
CODEN: HMGEE5; ISSN: 0964-6906

L4 ANSWER 29 OF 85 CAPLUS COPYRIGHT 2003 ACS
AU Mari, A; Amati, F.; Mingarelli, R.; Giannotti, A.; Sebastio, G.; Colloridi, V.; Novelli, G.; Dallapiccola, B.
TI Analysis of the elastin gene in 60 patients with clinical diagnosis of Williams syndrome
SO Human Genetics (1995), 96(4), 444-8.

L4 ANSWER 20 OF 85 CAPLUS COPYRIGHT 2003 ACS
AU Lindahl, Per; Karlsson, Linda; Hellstrom, Mats; Gebre-Medhin, Samuel; Willetts, Karen; Heath, John K.; Betsholtz, Christer
TI Alveogenesis failure in PDGF-A-deficient mice is coupled to lack of distal spreading of alveolar smooth muscle cell progenitors during lung development
SO Development (Cambridge, United Kingdom) (1997), 124(20), 3943-3953.

L4 ANSWER 40 OF 85 CAPLUS COPYRIGHT 2003 ACS
AU Ewart, Amanda K.; Morris, Colleen A.; Atkinson, Donald; Jin, Weishan; Sternes, Keith; Spallone, Patricia; Stock, A. Dean; Leppert, Mark; Keating, Mark T.
TI Hemizygosity at the elastin locus in a developmental disorder, Williams syndrome
SO Nature Genetics (1993), 5(1), 11-16.

L4 ANSWER 31 OF 85 CAPLUS COPYRIGHT 2003 ACS
AU Dallapiccola, B.; Amati, F.; Gennarelli, M.; Mari, A.; Novelli, G.
TI Advances in molecular analysis of congenital heart defects
SO Bulletin of Molecular Biology and Medicine (1995), 20(3,4), 135-140.

Shin-Lin Chen
AU 1632
CM1 12A15
Mail Box: CM1 12E12
(703) 305-1678

Development 124, 3943-3953 (1997)
Printed in Great Britain © The Company of Biologists Limited 1997
DEV4867

Alveogenesis failure in PDGF-A-deficient mice is coupled to lack of distal spreading of alveolar smooth muscle cell progenitors during lung development

Per Lindahl[1], Linda Karlsson[1], Mats Hellström[1], Samuel Gebre-Medhin[1], Karen Willetts[2,‡], John K. Heath[2] and Christer Betsholtz[1,*]

[1]Department of Medical Biochemistry and Microbiology, University of Göteborg, Medicinaregatan 9A, S-413 90 Göteborg, Sweden
[2]School of Biochemistry, University of Birmingham, Edgbaston, Birmingham B15 2TT, UK

*Author for correspondence (e-mail: Christer.Betsholtz@medkem.gu.se)
‡Present address: INSERM Unité 372, Campus de Luminy, Marseille 13276, Cedex 9, France

SUMMARY

PDGF-A$^{-/-}$ mice lack lung alveolar smooth muscle cells (SMC), exhibit reduced deposition of elastin fibres in the lung parenchyma, and develop lung emphysema due to complete failure of alveogenesis. We have mapped the expression of PDGF-A, PDGF receptor-α, tropoelastin, smooth muscle α-actin and desmin in developing lungs from wild type and PDGF-A$^{-/-}$ mice of pre- and postnatal ages in order to get insight into the mechanisms of PDGF-A-induced alveolar SMC formation and elastin deposition. PDGF-A was expressed by developing lung epithelium. Clusters of PDGF-Rα-positive (PDGF-Rα$^+$) mesenchymal cells occurred at the distal epithelial branches until embryonic day (E) 15.5. Between E16.5 and E17.5, PDGF-Rα$^+$ cells multiplied and spread to acquire positions as solitary cells in the terminal sac walls, where they remained until the onset of alveogenesis. In PDGF-A$^{-/-}$ lungs PDGF-Rα$^+$ cells failed to multiply and spread and instead remained in prospective bronchiolar walls. Three phases of tropoelastin expression were seen in the developing lung, each phase characterized by a distinct pattern of expression. The third phase, tropoelastin expression by developing alveolar SMC in conjunction with alveogenesis, was specifically and completely absent in PDGF-A$^{-/-}$ lungs. We propose that lung PDGF-Rα$^+$ cells are progenitors of the tropoelastin-positive alveolar SMC. We also propose that postnatal alveogenesis failure in PDGF-A$^{-/-}$ mice is due to a prenatal block in the distal spreading of PDGF-Rα$^+$ cells along the tubular lung epithelium during the canalicular stage of lung development.

Key words: mouse, lung, smooth mucle, alveogenesis, PDGF-A

INTRODUCTION

Platelet-derived growth factors are homo- or heterodimers of A- (PDGF-A) or B-chains (PDGF-B) that exert their action via binding to and dimerization of two types of receptor tyrosine kinases, α-receptors (PDGF-Rα) and β-receptors (PDGF-Rβ) (Heldin, 1992). PDGF was originally isolated from blood platelets as a growth factor for connective tissue and glial cells, but the two PDGF genes are now known to be expressed by a variety of cell types in developing, as well as in adult, vertebrates. The role of the PDGFs and their receptors during development has recently been studied using targeted gene inactivation in mice (Boström et al., 1996; Levéen et al., 1994; Lindahl et al., 1997; Soriano, 1994, 1997), using expressed dominant negative PDGF receptor mutants in *Xenopus* frogs (Ataliotis et al., 1995), and by application of neutralizing antibodies in *Lytechinus* sea urchins (Ramachandran et al., 1995) and in mice (Schatteman et al., 1996). Together these studies point to multiple roles of PDGFs and PDGF receptors at different stages of embryonic development, such as gastrulation (Ataliotis et al., 1995), cardiovascular development (Lindahl et al., 1997; Schatteman et al., 1996), and the development of kidney glomeruli (Levéen et al., 1994; Soriano, 1994). We recently showed that a proportion of mouse PDGF-A null mutants (PDGF-A$^{-/-}$) survive birth and develop generalized lung emphysema, involving the complete loss of alveolar smooth muscle cells (SMC) (Boström et al., 1996)*. Such cells, embedded in elastin fibres, normally build up the sphincter-like structures (alveolar ring muscles) around the openings of alveoli into alveolar ducts (Kapanchi and Gabbiani, 1997; Miller, 1921). The absence of alveolar SMC in PDGF-A$^{-/-}$ mice coincided with the loss of septal elastin deposits and failure of alveolar septal formation, suggesting a critical role of alveolar SMC in these processes. We also showed specific loss of scattered PDGF-Rα-positive cells in the lung parenchyma at embryonic day (E) 18.5 (plug scored E0.5; term=E19), and proposed that these cells were the progenitors of the alveolar

*In our previous publication (Boström et al., 1996) we used the term 'alveolar myofibroblasts' for the cells missing in PDGF-A-/- lung. This term has also been used for fibroblasts with contractile properties, which are abundant in the lung parenchyma (Kapanchi et al., 1974; Kapanchi and Gabbiani, 1997). However, there was no doubt that the cells specifically lost in PDGF-A-/- lungs were the smooth muscle cells normally situated at the entrance of the alveoli – the constituent cells of the alveolar ring muscles. In the present paper, we have therefore chosen to refer to them as 'alveolar smooth muscle cells'.

SMC (Boström et al., 1996). During embryonic development, lung epithelial tubular cells express PDGF-A, whereas mesenchymal cells express PDGF-Rα, indicating the existence of paracrine signalling between the epithelium and the mesenchyme (Boström et al., 1996; Orr-Urtreger and Lonai, 1992). The aim of the present study was to analyze how PDGF-A deficiency leads to failure of alveolar SMC formation during lung development. We hypothesized that alveolar SMC progenitors should express both PDGF-Rα and tropoelastin, and we have therefore studied in detail the expression patterns of these two genes, as well as the expression of smooth muscle α-actin and desmin, in developing wild-type and PDGF-A$^{-/-}$ lungs.

MATERIALS AND METHODS

Mice

PDGF-A$^{+/-}$ mice line #29 (Boström et al., 1996), bred as 129Ola/C57Bl6 hybrids, were crossed and embryos removed by Caesarean section at different embryonic ages. Tail or yolk sac tissue was used for genotyping by Southern blot analysis as described (Boström et al., 1996) or by a three-primer PCR. The forward primer 5′CCTTTGGCTCTAGGGTGGAATTTC and the two reverse primers 5′TGGATGTGGAATGTGTGCGAG and 5′ACACGAATGAACAGGGATGGG yielded 470 bp wild type and 368 bp mutant allele products in a 40-cycle reaction (96°C for 30 seconds, 55°C for 30 seconds, 65°C for 3 minutes).

In situ hybridization

We used a modification of a protocol described for non-radioactive in situ hybridization (Boström et al., 1996; Henrique et al., 1995). Briefly, embryos were fixed overnight in 4% buffered paraformaldehyde (PFA), infiltrated with 30% sucrose, 0.02% sodium azide, embedded in OCT compound, cryo-sectioned, and stored at −80°C. Prior to hybridization, sections were treated with 10 μg/μl of Proteinase K and refixed in PFA for 15 minutes. Prehybridization occurred in a solution containing 50-55% (55% were used for PDGF-B- and PDGF-Rα-probes, 50% for the others) deionized formamide, 10% dextran sulphate, 1 mg/ml yeast tRNA, 1× Denhardt's solution, 5 mM EDTA, 0.2 M NaCl, 0.013 M Tris-HCl, 5 mM NaH_2PO_4, 5 mM $NaHPO_4$, pH 7.5. Pre-heated probes (see below) were added at a concentration of 3-8 μg/ml hybridization solution, and the sections were incubated overnight. Post-hybridization washes were carried out in 1× SSC, 50-55% formamide and 0.1% Tween 20. The entire process from pre- to post-hybridization was performed at 65-72.5°C (72.5°C were used for PDGF-B- and PDGF-Rα-probes, 65°C for the others). Digoxygenin (DIG)-labelled RNA probes, and their detection on sections using an alkaline phosphatase-conjugated antibody, was done using DIG-labelled UTP, the 'DIG RNA labelling kit' and the 'DIG nucleic acid detection kit' (Boehringer Mannheim), according to the manufacturer's instructions.

DNA-probes

PDGF-B sense and antisense probes were generated from a 800 bp mouse cDNA containing the full length coding sequence cloned in pBS-SK (kindly provided by Dr P. Soriano). PDGF-Rβ probes were generated from a 461 bp *Sac*I fragment cloned in pGEM-2 (kindly provided by Dr J. Escobedo). PDGF-A probes were generated from a 900 bp *Eco*RI fragment cloned in pGEM-1 (kindly provided by Dr W. D. Richardson). Two PDGF-Rα fragments, a 917 bp *Eco*RI-*Eco*RV and a 719 bp *Eco*RV-*Eco*RI fragment, were cut out from a receptor extracellular domain-encoding 1.6 kbp *Eco*RI fragment (kindly provided by Dr W. D. Richardson), subcloned into pBS-SK, and used for probe generation. Probes against tropoelastin mRNA were generated from a 1.1 kbp *Eco*RI rat cDNA fragment cloned into pBS (kindly provided by Dr J. Foster) and a 644 bp *Bam*HI-*Kpn*I mouse cDNA fragment cloned into pBS-SK. The mouse cDNA were obtained by RT-PCR on postnatal lung tissue, using a forward primer 5′TTATCCCATCAAAGCACC and reverse primer 5′AACCCCACCAACACCAACTC, which yielded a 895 bp fragment. We show the use of antisense probes on 14 μm thick sections. As negative controls, the corresponding sense probes were used. No consistent hybridization signals were obtained with any of the sense probes (data not shown). Photography was done in a Nikon microphot-FXA microscope. Unstained sections in combination with Nomarski optics were used to allow for good sensitivity and resolution.

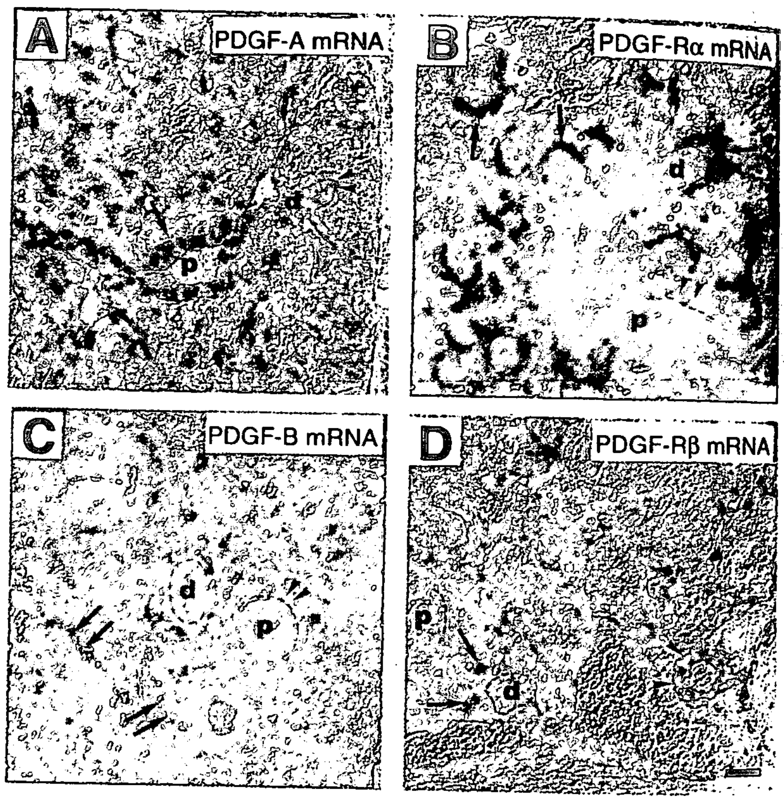

Fig. 1. PDGF and PDGF receptor expression patterns in the developing lung. Non-radioactive in situ hybridization (positive reaction indicated by blue stain) of sections from E14.5 wild-type lungs. Examples of proximal (p) and distal (d) tubules are shown, where the basal epithelial surface is indicated by a dotted line. (A) PDGF-A is expressed by epithelial cells of both proximal and distal tubules. Non-labelled cells could be found (arrows) intermingled with strongly labelled cells in the proximal tubules, while epithelial cells of distal tubules (acinar tubules) were uniformly strongly labelled (arrowheads). (B) PDGF-Rα is strongly expressed by 1-2 layers of clustered mesenchymal cells (arrows) lining the distal epithelial tubules (d) or epithelial buds. Proximal epithelial tubules are lined by cells showing weak PDGF-Rα expression (arrowheads). (C) PDGF-B is expressed by mesenchymal cells located at some distance from the epithelial cells (arrowheads). Erythrocytes (arrows) are often surrounded by PDGF-B-positive cells, consistent with an endothelial expression of PDGF-B. (D) PDGF-Rβ is expressed by mesenchymal cells clustered in arterial walls (arrowheads), or scattered in blood capillary-containing regions of the mesenchyme (arrows). Bar, 80 μm.

Immunohistochemistry

Immunohistochemistry was performed using antibodies directed against smooth muscle α-actin (clone 1A4; Dako) and desmin (clone D33; Dako), according to protocols supplied by the manufacturer.

RESULTS

PDGF-A and PDGF-Rα expression patterns in the developing lung

PDGF-A mRNA is expressed by many types of epithelium during embryonic development (Orr-Urtreger and Lonai, 1992). In the E14.5-16.5 developing lung, we found that PDGF-A mRNA was expressed in the epithelial tubules of both proximal and distal location (Fig. 1A). The patterns were slightly different at the two locations; in proximal (developing bronchial) epithelium, there was a mixture of strongly labelled cells with weakly or non-labelled cells. At distal locations (the acinar tubules), the epithelial labelling for PDGF-A was uniformly strong.

PDGF-Rα mRNA is expressed in lung mesenchyme from the onset of lung development (Orr-Urtreger and Lonai, 1992, and data not shown). At E14.5-15.5, strong expression of PDGF-Rα was seen in the 1-2 layers of mesenchymal cells surrounding the distal epithelial branches and terminal buds (Fig. 1B) (strongly PDGF-Rα-positive cells are hereafter referred to as PDGF-Rα$^+$ cells). Weaker but significant PDGF-Rα expression was also seen in the mesenchyme surrounding the proximal epithelium of prospective bronchi and bronchioles.

Since alveolar SMC are specifically absent in postnatal PDGF-A$^{-/-}$ mice (Boström et al., 1996), and since PDGF-Rα is the only known receptor for PDGF-A (Heldin, 1992), we assumed that the alveolar SMC progenitors should carry PDGF-Rα. We suspected that the PDGF-Rα$^+$ cells at the terminal buds could be such progenitors and therefore compared the PDGF-Rα expression patterns in PDGF-A$^{-/-}$ and PDGF-A$^{+/+}$ lungs. At E14.5-15.5, these patterns were indistinguishable (Fig. 2A,B), but at E16.5 and later, they differed significantly (Fig. 2C-L). In E16.5 PDGF-A$^{+/+}$ lungs, PDGF-Rα$^+$ cells were more numerous and appeared to be more spread compared to the PDGF-A$^{-/-}$ lung, in which their distribution was essentially unchanged from E15.5 (Fig. 2C,D). At

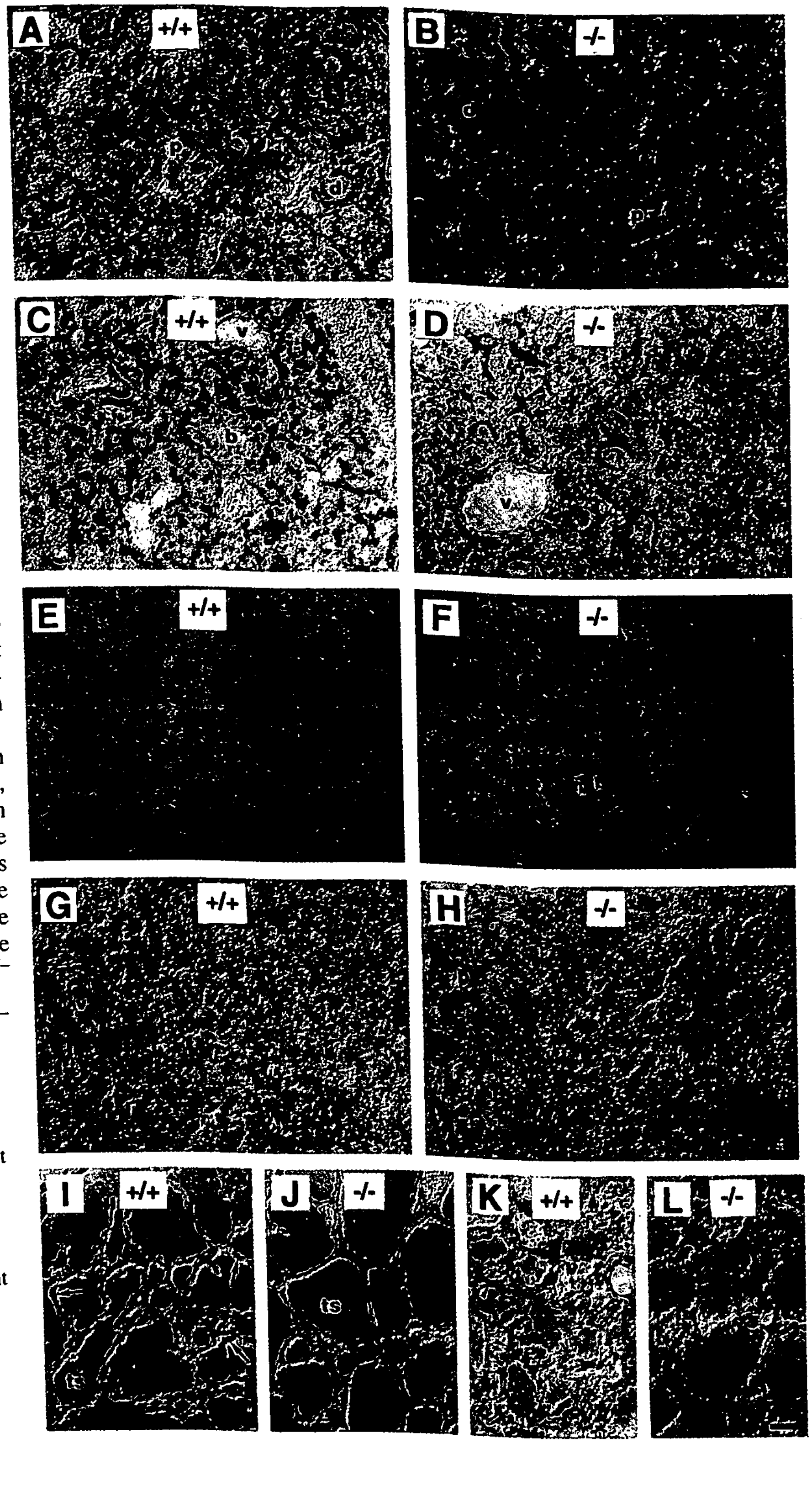

Fig. 2. PDGF-Rα expression patterns in developing wild-type and PDGF-A$^{-/-}$ lungs. PDGF-Rα expression was compared at E15.5 (A,B), E16.5 (C,D), E17.5 (E-H), P1 (I,J) and P7 (K,L). p, proximal tubule; d, distal tubule, b, bronchiole; v, blood vessel; ts, terminal sac. Arrowheads in F point at clustered PDGF-Rα$^+$ cells at proximal tubules. Arrows in I and arrowheads in K point at scattered PDGF-Rα$^+$ cells situated in the walls of alveolar sacs. Note that scattered PDGF-Rα$^+$ cells are fewer in E16.5-17.5 PDGF-A$^{-/-}$ lungs and virtually absent in postnatal lungs compared with wild-type (+/+) littermate controls. The presence of erythrocytes in the alveolar sacs of postnatal lungs is due to aspiration of blood following decapitation of the animal. Bar, 80 μm (160 μm for E and F, which show an overview of the E17.5 lung).

E17.5 PDGF-Rα^{+} cells appeared completely scattered in the PDGF-A$^{+/+}$ lung; at this time most of them occurred as solitary cells lining the lumen of the prospective terminal sacs (Fig. 2E-H). Weak staining for PDGF-Rα was also seen in vascular walls and in cells surrounding the epithelium at more proximal sites; in prospective bronchial and bronchiola... In E17.5 PDGF-A$^{-/-}$ lungs on the other hand, the appea... of numerous scattered PDGF-Rα^{+} cells was not seen... regions where thin-walled tubules of the prospective termi... sacs dominated, hardly any PDGF-Rα^{+} cells could be fo...

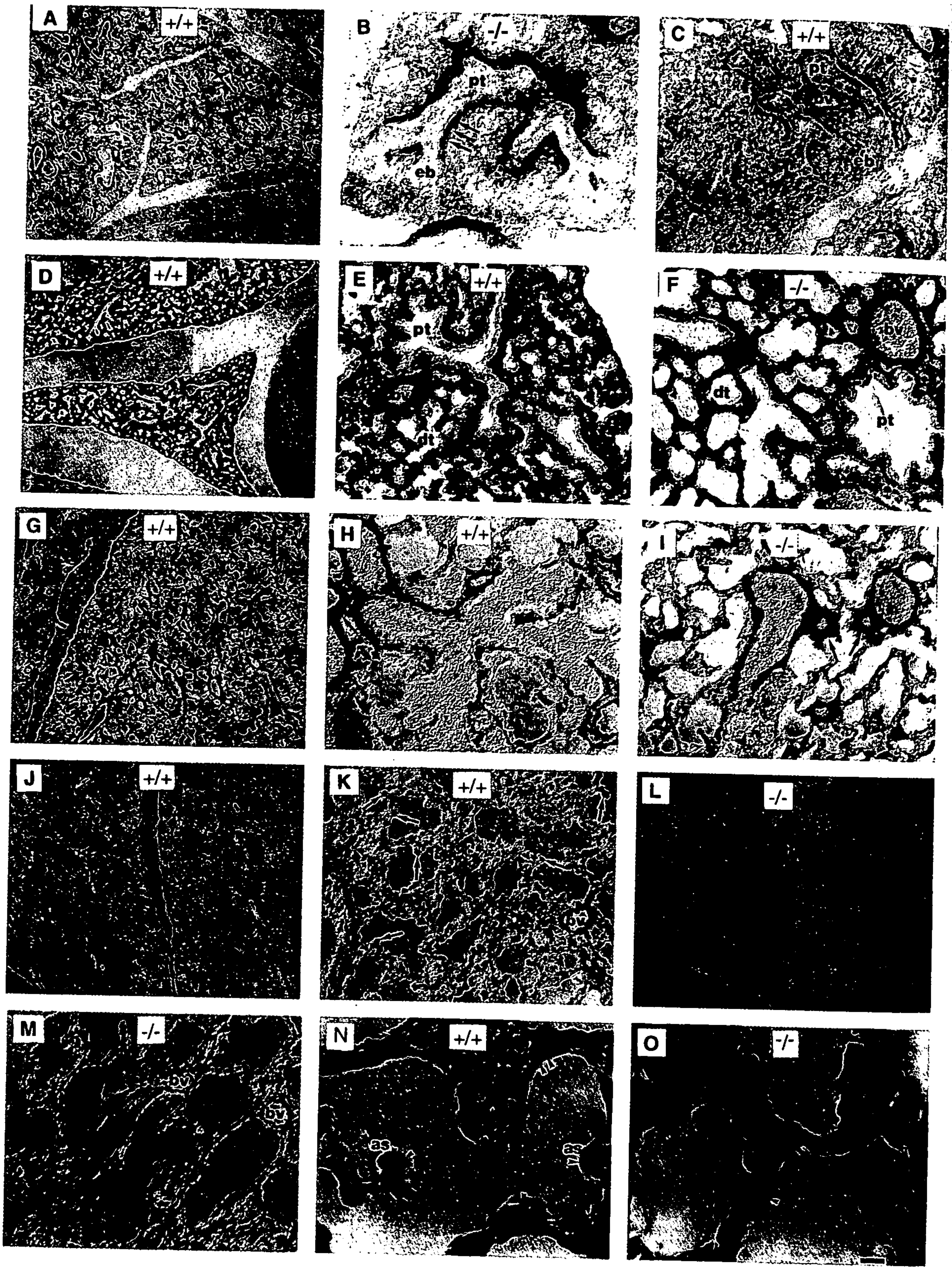

(Fig. 2F,H). Instead, the few PDGF-Rα$^+$ cells seen in E17.5 lungs were situated in small clusters at more proximal epithelial tubules (Fig. 2F,H). At E18.5 and postnatal day (P)1, the difference between PDGF-Rα expression patterns in PDGF-A$^{+/+}$ and PDGF-A$^{-/-}$ lungs was pronounced in that no, or very few, PDGF-Rα$^+$ cells were seen in the walls of terminal sacs in PDGF-A$^{-/-}$ lungs, whereas such cells were numerous in PDGF-A$^{+/+}$ lungs (Fig. 2I,J). At P4-P7 the density of scattered PDGF-Rα$^+$ cells declined in the PDGF-A$^{+/+}$ lung, suggesting down-regulation of PDGF-Rα in differentiated cells (Fig. 2K). PDGF-A$^{-/-}$ lungs lacked PDGF-Rα$^+$ cells also at P4-7 (Fig. 2L). The weak PDGF-Rα expression was similar in PDGF-A$^{+/+}$ and PDGF-A$^{-/-}$ lung tissue, and occurred typically in developing bronchial and vascular walls. This expression remained in the early postnatal lungs but declined before P7.

Tropoelastin expression and elastin deposition in developing normal and PDGF-A-deficient lungs

Elastin deposition in the alveolar septum is believed to be accomplished by interstitial myofibroblast-like cells (Collett and Des Biens, 1974; Fukuda et al., 1983; Noguchi and Samaha, 1991; Vaccaro and Brody, 1978), but the exact identity of the elastin-producing cell(s) has remained unclear, considering the presence of three types of contractile mesenchymal cells in the alveolar septum: the alveolar ring SMC, alveolar myofibroblasts and microvascular pericytes (Kapanchi and Gabbiani, 1997). We therefore studied the tropoelastin mRNA expression pattern in PDGF-A$^{+/+}$ and PDGF-A$^{-/-}$ embryonic and postnatal lungs. At E15.5, expression of tropoelastin mRNA was confined to mesenchymal cells lining the proximal tubules, apparently leaving the buds free from deposited elastin (Fig. 3A-C). At E18.5, when branching of the lung is terminated (Hilfer, 1996), essentially all of the lung mesenchyme was strongly tropoelastin-positive (Fig. 3D-F). Tropoelastin expression was also abundant in the developing vasculature, and was seen both in vascular endothelium and in the developing vascular wall (Fig. 3E,F,K,M). Postnatally, the lung tropoelastin expression became progressively restricted to a subset of interstitial cells. Already on P1 the general mesenchymal expression of tropoelastin mRNA was significantly down-regulated (Fig. 3G-I), and later, at P7-P14, expression was limited to a scattered population of mesenchymal cells having the expected location of alveolar SMC progenitors (Fig. 3J,K), namely at the edge of growing alveolar septa, and to developing vascular and bronchial wall cells. In PDGF-A$^{-/-}$ lungs, the tropoelastin expression pattern at prenatal ages was similar to that of PDGF-A$^{+/+}$ lungs (Fig. 3C,F,I). Postnatally, however, there was complete and selective loss of the scattered mesenchymal tropoelastin-positive cells in the PDGF-A$^{-/-}$ lungs (Fig. 3L,M), whereas the vascular and bronchial wall expression was indistinguishable in PDGF-A$^{+/+}$ and PDGF-A$^{-/-}$ lungs (Fig. 3J,L).

The deposition of elastin fibres was studied using van Gieson-elastin staining of tissue sections. Before P4, i.e. before the onset of alveogenesis, no difference could be discerned between PDGF-A$^{+/+}$ and PDGF-A$^{-/-}$ lungs (data not shown). For example, in the wall of the prealveolar sacs at P4, elastic fibres were seen of the same abundance and thickness in both genotypes. After onset of alveogenesis a dramatic difference was noticed, however; the elastin deposition associated with alveolar septum formation did not occur in PDGF-A$^{-/-}$ lungs (Fig. 3N,O).

Fig. 3. Tropoelastin expression in developing lungs. Non-radioactive in situ hybridization of wild-type (+/+; A,C,D,E,G,H,J,K,N) and PDGF-A$^{-/-}$ (B,F,I,L,M,O) sections. (A-C) In E15.5 (B) and E16.5 (A,C) lungs, mesenchymal cells adjacent to the epithelial tubules produce tropoelastin mRNA. Expression is intense in mesenchymal cells (arrows) lining the proximal epithelial tubules (pt), while the mesenchyme surrounding the epithelial buds (eb) is devoid of tropoelastin expression. Tropoelastin mRNA is also produced by endothelial and SMC progenitors in blood vessels (bv). In E15.5-16.5 lungs, tropoelastin expression does not seem to be affected by PDGF-A deficiency. (D-F) At E18.5 tropoelastin mRNA is produced by all mesenchymal cells in the lung, at proximal (pt) as well as distal (dt) sites, and in blood vessel (bv) endothelial and SMC cells. PDGF-A deficiency did not affect this second phase of tropoelastin expression. (G-I) Postnatally, at P1, the general expression of tropoelastin mRNA is significantly reduced, and most mesenchymal cells are weakly stained. The high level of expression is maintained in blood vessels (arrows). (J-M) At P7, a population of scattered mesenchymal cells, typically located at the tips of ingrowing alveolar septa (arrows), express tropoelastin. The scattered tropoelastin-positive cells are completely absent in PDGF-A$^{-/-}$ lungs (L,M). The presence of tropoelastin expressing blood vessels (bv) in PDGF-A$^{+/+}$ and PDGF-A$^{-/-}$ lungs provides an internal control of hybridization efficiency. (N,O) Elastin fibers (arrowheads), visualised by van Gieson-elastin staining, are deposited in bundles in the alveolar septa (arrows) of P20 PDGF-A$^{+/+}$ lungs. Consistent with the total absence of scattered tropoelastin producing cells in the alveolar sac walls of PDGF-A$^{-/-}$ lungs, elastin fibers are dramatically reduced in number in the P20, PDGF-A$^{-/-}$ lungs. The presence of erythrocytes in the alveolar sacs of postnatal lungs is due to aspiration of blood following decapitation of the animal. Bar, 320 μm for A,D,G,J,L; 80 μm for C,E,F,H,I,K,M; 60 μm for B and 25 μm for N and O.

PDGF-Rα and tropoelastin expression do not overlap in the alveolar SMC lineage

The lack of distal spreading of PDGF-Rα$^+$ cells seen prenatally correlates with the later occurring absence of tropoelastin-producing cells in growing alveolar septa as well as with the subsequent lack of mature alveolar SMC. We assumed that these cells represent the same lineage, in which PDGF-Rα expression preceeds that of tropoelastin. In P4 PDGF-A$^{+/+}$ lungs (at the onset of alveogenesis), both PDGF-Rα and tropoelastin were expressed in mesenchymal cells occurring at roughly the same abundance (Fig. 4). However, whereas the tropoelastin-positive cells were preferentially associated with epithelial folds typical of forming alveolar septa (Fig. 4A,B), this localization was not apparent for the PDGF-Rα$^+$ cells, which were scattered, but not preferentially located to forming alveolar septa (Fig. 4C,D). Although a few PDGF-Rα$^+$ cells appear to localize to forming alveolar septa (arrow in Fig. 4C), the divergent expression patterns are consistent with down-regulation of PDGF-Rα expression immediately prior to, or following, the onset of tropoelastin expression in alveolar SMC progenitors. Lack of overlapping expression of PDGF-Rα and tropoelastin was seen also at P7 when alveogenesis had proceeded further, by which time fewer PDGF-Rα$^+$ cells, but a larger number of tropoelastin-positive cells, were seen compared to P4, and where preferential location of the tropoelastin-positive, but not the PDGF-Rα$^+$ cells, occurred in developing alveolar septa (compare Figs 2K and 3K). Tropoelastin and strong PDGF-Rα expression was also not overlap-

ping at the pseudoglandular stage (compare Figs 2A and 3C); at this time PDGF-Rα expression occurred in distal mesenchyme and tropoelastin expression in proximal mesenchyme.

Smooth muscle α-actin expression in the developing mouse lung

Prenatally, smooth muscle α-actin was expressed in prospective bronchial, bronchiolar and vascular walls (Fig. 5A-D) but not in the PDGF-Rα$^+$ mesenchyme at the terminal buds. This pattern was indistinguishable in PDGF-A$^{+/+}$ and PDGF-A$^{-/-}$ lungs. Postnatally, a similar location of smooth muscle α-actin-positive cells was seen; positive cells occurred in bronchi and large blood vessels (not capillaries), but did not show a scattered distribution similar to that of PDGF-Rα$^+$ or tropoelastin-positive cells (Fig. 5E-H and data not shown). We have shown previously that smooth muscle α-actin is expressed in alveolar SMC once alveogenesis is completed, from approximately 3 weeks of postnatal age (Boström et al., 1996). However, at this age, PDGF-Rα or tropoelastin were no longer expressed in these cells (data not shown). It appears that the expression of smooth muscle α-actin occurs relatively late in the ontogeny of alveolar SMC, i.e. in alveolar ring muscles only once the process of alveogenesis is completed, but is already seen in bronchial or vascular wall SMC prenatally.

Although smooth muscle α-actin did not label specifically the alveolar SMC cell lineage, abnormal vascular expression of this protein was revealed in the P14 PDGF-A$^{-/-}$ lung. Here, the expression was strongly up-regulated in arterioles (Fig. 5H). We have shown previously that 3-week-old PDGF-A$^{-/-}$ pups have right-sided cardiac myocardium hypertrophy (Boström et al., 1996). It is possible that both these phenotypes reflect the same secondary changes in the lung, rather than being primarily caused by PDGF-A deficiency.

Desmin expression in the developing mouse lung

Desmin has been suggested as a marker for alveolar ring muscles and alveolar myofibroblasts (Kapanchi and Gabbiani, 1997). We found that desmin was expressed in a large proportion of mesenchymal cells in the developing pre- and postnatal lung. This expression pattern did not specifically overlap with that of PDGF-Rα or tropoelastin after P2. No apparent differences were noticed between the desmin expression patterns in PDGF-A$^{+/+}$ and PDGF-A$^{-/-}$ lungs at prenatal or postnatal ages (Fig. 5F-O). We conclude that desmin is not a specific marker for alveolar SMC progenitors, but shows an expression pattern and distribution consistent with alveolar myofibroblasts, or possibly microvascular pericytes. Whereas both alveolar SMC and myofibroblasts have been suggested to be desmin positive by others, lung pericytes were suggested to be negative (Kapanchi and Gabbiani, 1997). In this study, desmin was also found in bronchial epithelial cells, specifically located to the ciliae (Fig. 5N).

PDGF-B and -Rβ expression patterns in the developing lung

As shown above, the expression patterns of PDGF-A and -Rα mRNA in the developing lung suggest that a PDGF-A-containing PDGF dimer released by lung epithelial cells promotes spreading of PDGF-Rα-positive progenitor cells. Since PDGF-B can bind to and activate PDGF-Rα and since PDGF-B can form heterodimers with PDGF-A, it was of interest to see if PDGF-B was expressed in the developing lung. By in situ hybridization, PDGF-B was shown to be expressed in a subset of cells in the lung mesenchyme (Fig. 1C). At E14.5 these cells locate to a region outside the clusters of PDGF-Rα-positive mesenchymal cells, and appear at sites where extensive blood vessel formation takes place (Ten Have-Opbroek, 1981). We have recently shown that PDGF-B is expressed by capillary and small arteric endothelial cells in many tissues of the mouse embryo, including the lung, as well as in fetal liver megakaryocytes (Lindahl et al., 1997). The absence of any overlap between PDGF-A and -B expression in the developing lung suggests that the lung epithelium produces PDGF-AA dimers and the lung capillary endothelium produces PDGF-BB dimers, and that no PDGF-AB dimers are formed. It is clear from the PDGF-A null phenotype that the PDGF-Rα-positive alveolar ring SMC require PDGF-AA. Whether they also require endothelium-derived PDGF-BB is at present not clear, but studies of the spreading of PDGF-Rα-positive lung mesenchymal cells in E17.5-18.5 PDGF-B knockout embryos should answer this question.

PDGF-Rβ was expressed in yet another subset of mesenchymal cells, these being either located in the developing lung arteric

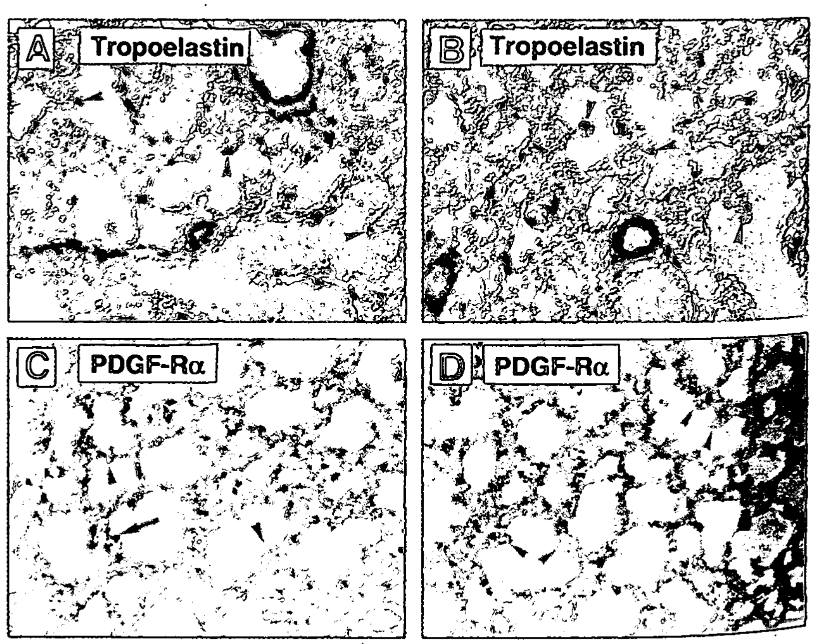

Fig. 4. Tropoelastin and PDGF-Rα expression at P4.5. Two representative areas of lung tissue are shown for each hybridization. Close comparison of the expression patterns reveal that most tropoelastin-positive cells (arrowheads indicate examples in A and B) are located to growing alveolar septa, whereas most PDGF-Rα$^+$ cells did not have an apparent localization to alveolar septa (arrowheads in C and D). A few PDGF-Rα$^+$ cells were seen in association with structures that may be alveolar septa, as indicated by the arrow in C. Bar, 80 μm.

walls, or intermingled with the PDGF-B-positive cells and having a scattered location (Fig. 1D). This pattern is distinctly different from that of the PDGF-Rα expression, since the PDGF-Rβ-positive cells are already scattered in the lung mesenchyme at E14.5, i.e. during the pseudoglandular stage, at which PDGF-Rα expression occurs in clusters of mesenchymal cells at the epithelial buds (Fig. 1B). We have recently shown that developing microvascular pericytes in other locations express PDGF-Rβ and spread along sprouting capillary endothelium in a PDGF-B-dependent manner (Lindahl et al., 1997). Indeed, the PDGF-Rβ-positive cells in the lung also require PDGF-B for spreading (Lindahl et al., 1997, and data not shown). It is therefore likely that the scattered lung PDGF-Rβ-positive cells represent developing microvascular pericytes. In summary, the two genes encoding the constituent chains of PDGF ligands and the two PDGF receptor genes are all expressed in the developing mouse lung, probably in different cell types, as schematically illustrated in Fig. 6.

DISCUSSION

Epithelial-mesenchymal interactions in lung development

Four stages of lung development can be

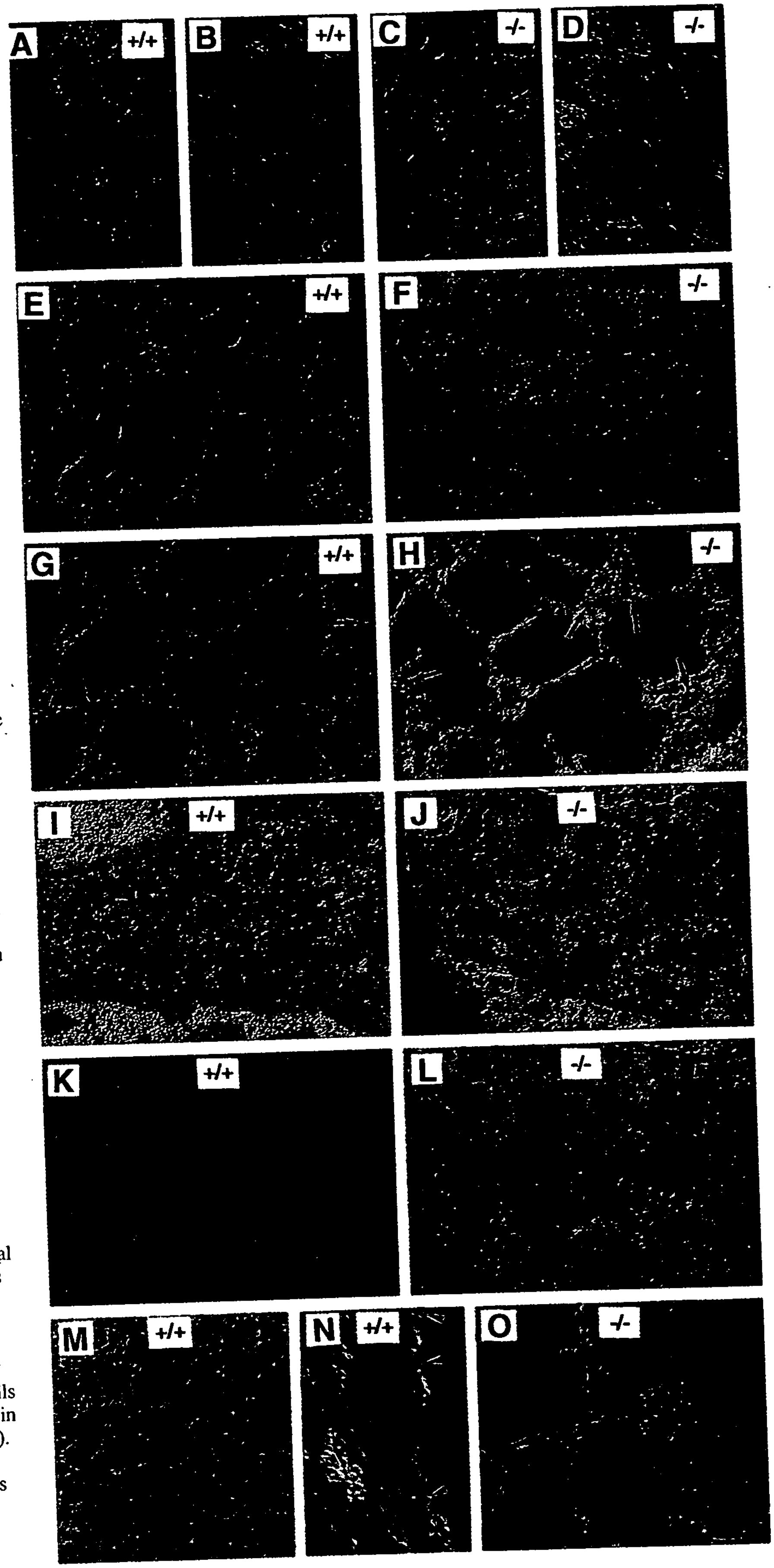

Fig. 5. Smooth muscle α-actin and desmin expression in developing lungs. Smooth muscle α-actin immunohistochemistry is shown for E15.5 (A-D), P1 (E,F) and P14 (G,H) lungs. Expression in seen in bronchial (b) and blood vessel (v) walls and in the mesenchyme surrounding proximal tubular epithelium (p) (arrows in B and D) but not distal epithelium (d) (arrowheads in B and D). Thus smooth muscle α-actin expression does not occur at detectable levels in the PDGF-Rα+ mesenchyme, which is situated surrounding the distal epithelium and the epithelial buds (see Figs 1 and 2). No difference was noticed between the patterns of expression of smooth muscle α-actin in wild-type (+/+) or PDGF-A$^{-/-}$ lungs. At P14, smooth muscle α-actin was up-regulated in arterioles of the emphysematous PDGF-A$^{-/-}$ lung (compare G with H; arterioles indicated by arrows). Desmin immunohistochemistry is shown for E 15.5 (I,J), P1 (K,L) and P14 (M-O). At E15.5, desmin expression occurs in mesenchymal cells at some distance from the epithelial tubules (examples of basal epithelial surfaces are indicated by dotted lines), thus coinciding with the region where extensive blood capillary formation takes place and where PDGF-B and PDGF-Rβ expression occurs. Thus desmin expression does not seem to occur in the PDGF-Rα$^+$ cells (see Figs 1 and 2). The tropoelastin-positive cells situated in developing alvoelar septa were also desmin negative, or expressed very low levels of desmin (M). No difference was apparent between the desmin expression patterns in wild-type or PDGF-A$^{-/-}$ lungs at prenatal or early postnatal ages. Desmin is also expressed in the ciliae of bronchial epithelial cells (N, arrowheads). Bar, 80 μm (40 μm for N).

discerned, based on histological appereance (Ten Have-Opbroek, 1981, 1991). During the pseudoglandular stage (E9.5-E16.6 in the mouse) the primitive lung bud forms the basic pattern of bronchi through dichotomous branching (Hilfer, 1996). This branching appears to be induced by the mesenchyme surrounding the distal ends of the epithelial tubules. During the canalicular stage (E16.6-E17.4 in the mouse), the terminal respiratory portion of the lungs is established through continued centrifugal branching. Moreover, the epithelial cells lining the prospective terminal sacs develop a flattened appereance, and close contacts are formed between blood vessels and the developing respiratory units. The terminal sac stage (E17.4-P5 in the mouse) is characterized by expansion of the terminal tubules into sacs with a flat epithelium composed of differentiated pneumocytes. The last stage, alveogenesis, is initiated postnatally (starting approximately at P5 in the mouse) by the formation of alveolar septa.

Epithelial-mesenchymal reciprocal signalling is known to occur during the development of many parenchymal organs. For example, the role of the distal lung mesenchyme for inducing branch formation is well established (Alescio and Cassini, 1962; Goldin et al., 1984; Goldin and Wessels, 1979; Hilfer, 1996; Wessels, 1970). How this signalling is governed at the molecular level is not fully clear, but a number of molecules have been implicated. Transgenic overexpression, or misexpression, of bone morphogenetic protein-4 (Bellusci et al., 1996), sonic hedgehog (Bellusci et al., 1997), transforming growth factor (TGF)-α (Korfhagen et al., 1994), TGF-β1 (Zhou et al., 1996) or fibroblast growth factor (FGF)-7 (Simonet et al., 1995) lead to defects in lung development. Inhibition of FGF-receptor signalling by expression of dominant negative FGF-R2 inhibits branching beyond two main bronchi (Peters et al., 1994). Involvement of transforming growth factor-β members in lung development is also suggested from the knockout of TGF-β3 (Kaartinen et al., 1995) and from in vitro studies of the effect of TGF-β1 on lung epithelial branching (Serra et al., 1994). Epidermal growth factor receptor (EGFR) signalling is implicated in lung development since EGFR null mice display abnormal lung development (Miettinen et al., 1995).

The lung defect seen in PDGF-A$^{-/-}$ mice combined with the normal developmental expression of PDGF-A and its receptor, suggest that paracrine PDGF-A – PDGF-Rα receptor signalling constitutes a critical part of the epithelial-mesenchymal signalling in the developing lung, and that epithelial-mesenchymal interaction in the lung is also important for functions other than branch initiation. Specifically, the present work suggests that when the final bronchial branches are induced, epithelial cell signalling involving PDGF-AA is essential for a subset of mesenchymal cells to multiply and move to a new, more distal location, at which they can complete the last stage of lung morphogenesis: alveogenesis.

PDGF-A dependent multiplication and spreading of PDGF-Rα+ cells in the developing lung

PDGF-A is expressed in the tubular epithelium during the pseudoglandular stage. At this stage strong PDGF-Rα expression occurs in mesenchymal cells surrounding the end buds and the distal parts of the same tubules. During the canalicular stage an important change occurs in the distribution of the PDGF-Rα^+ cells as they spread along the surface of the prospective terminal sacs. The scattered PDGF-Rα^+ cells remain in this position until the onset of alveogenesis, at which time the PDGF-Rα mRNA is down-regulated. The details of the expression patterns in PDGF-A$^{+/+}$ compared to PDGF-A$^{-/-}$ animals suggests that the specific absence of the scattered PDGF-Rα^+ cells in PDGF-A$^{-/-}$ lungs is due to a block in proliferation and distal spreading of these cells. PDGF-A$^{-/-}$ lungs contain far fewer PDGF-Rα^+ cells at E17.5, but in addition, the remaining cells occur mainly at a proximal location, lining prospective bronchioles, and little if any scattering of PDGF-Rα^+ cells is seen. These observations are consistent with a model where PDGF-Rα^+ cells lining the acinar tubules relocate from this site to the epithelial surface of the prospective terminal saccules in response to PDGF-AA (Fig. 7). In the absence of PDGF-AA, spreading does not occur, and conse-

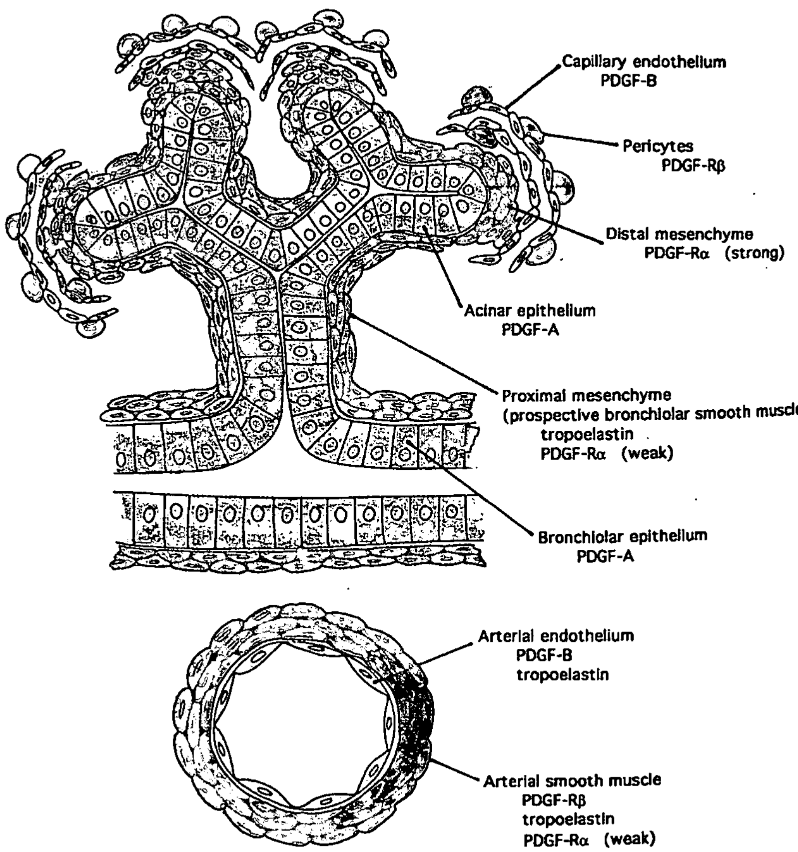

Fig. 6. PDGF, PDGF receptor and tropoelastin expression in the developing lung. Schematical illustration of expression sites at the pseudoglandular stage of lung development in proximal and distal epithelial tubules and associated mesenchyme and in lung arteries and arterioles. The following cell types are shown in different colours: vascular endothelium (yellow), lung epithelium (grey), vascular wall SMC progenitors (red), bronchiolar SMC progenitors (green) and alveolar SMC progenitors (blue).

quently the PDGF-Rα^+ cells remain at proximal (bronchiolar) sites along the epithelial branches. The failure of spreading of PDGF-Rα^+ cells may therefore reflect the lack of PDGF-AA-induced cell proliferation and migration. The proposed model would also be compatible with alternative, or additional, functions of PDGF-A such as regulation of cell survival and differentiation. However, we found no histological evidence of increased apoptosis in PDGF-A$^{-/-}$ lungs, and undetectable apoptosis by TUNEL labelling in wild-type or PDGF-A$^{-/-}$ lungs (data not shown). This appears consistent with the previously reported very low apoptosis frequency in the late mouse embryonic lung (Bellusci et al., 1997, 1996).

The PDGF-Rα^+ cells are probably alveolar SMC progenitors

Because of the lack of overlapping markers, we have failed to produce direct evidence that the PDGF-Rα^+ cells that spread distally at the canalicular stage of lung development are indeed the progenitors of the tropoelastin-positive cells actively involved in the process of alveogenesis from P4, and the later occurring smooth muscle α-actin-positive alveolar SMC. Our assumption that these cells represent the same cell lineage, and consequently that PDGF-Rα is down-regulated at the onset of tropoelastin expression and alveogenesis, is, however, strongly supported by several pieces of indirect evidence. The absence of scattered PDGF-Rα^+ cells in PDGF-A$^{-/-}$ lungs from E17.5 correlates with the absence of scattered tropoelastin-expressing cells from P4, as well as with the specific and complete absence of differentiated alveolar SMC at 3 weeks. By transmission electron microscopy, no other cells but the alveolar SMC were found to be missing in the PDGF-A$^{-/-}$ lung (Boström et al., 1996). These studies did not address the abundance of alveolar myofibroblasts and pericytes, but the desmin stainings shown here suggest that the alveolar myofibroblast compartment is unaffected. Pericytes are also probably not affected since pericyte loss leads to vascular leakage, microaneurysm formation and hemorrhage, as occurs in PDGF-B$^{-/-}$ mice (Lindahl et al., 1997) but not in PDGF-A$^{-/-}$ mice. The spatial distribution and abundance of PDGF-Rα^+ cells in PDGF-A$^{+/+}$ lungs are in agreement with a role in alveogenesis. It is also reasonable to predict that a cell type (or its progenitor) that is specifically lost in PDGF-A-deficient mice should carry the receptor for PDGF-A at a stage in development when PDGF-A is expressed and also be located close to the source of ligand, as is the case for the PDGF-Rα^+ mesenchymal cells discussed.

Role of PDGF-A in lung elastogenesis

Elastin is the major extracellular matrix constituent of the lung, making up approximately 25% of the dry weight of the adult lung. The tropoelastin mRNA expression patterns in developing PDGF-A$^{+/+}$ and PDGF-A$^{-/-}$ lungs reveal three phases of lung elastogenesis, brought about in part by different cell types, and showing different dependence on PDGF-A/Rα signalling. At the pseudoglandular stage, elastin is expressed in mesenchyme apposed to the proximal lung epithelium, whereas the distal mesenchyme, which is PDGF-Rα positive, lacks tropoelastin expression at this stage (Fig. 3 A-C). Considering the polarised expression of tropoelastin, and the different properties of proximal and distal mesenchyme for inducing branch formation (Heine et al., 1990; Hilfer et al., 1985), elastin fibers deposited at proximal sites may be important for prevention of ectopic branching of the lung epithelium. Conversely, the lack of elastin deposition at the buds during the pseudoglandular stage may permit further branching. This first phase of lung elastogenesis is unaffected by the absence of PDGF-A. During the terminal sac stage, at which time epithelial branching has ceased, tropoelastin is strongly expressed by a majority of lung mesenchymal cells both at proximal and distal sites, apparently including smooth muscle progenitors as well as lung fibroblasts. This expression likely leads to deposition of elastic fibres in the walls of the terminal sac s, which provides sufficient elasticity in these structures to allow for efficient breathing during the first postnatal days. This second phase of lung elastogenesis is not detectably influenced by the absence of PDGF-A. The third phase involves deposition of elastin in alveolar septa by prospective alveolar SMC, a process intimately coupled to alveolar septation. This phase shows an obligatory requirement for PDGF-A. The hypothesis has been put forward that elastin deposition by alveolar cells provides a critical driving force in the morphogenesis of alveolar septa, based on morphological studies of lung development (Burri and Weibel, 1977; Emery, 1970; Noguchi et al., 1989). Our data support this hypothesis by correlating the loss of alveolar septal elastin deposition with

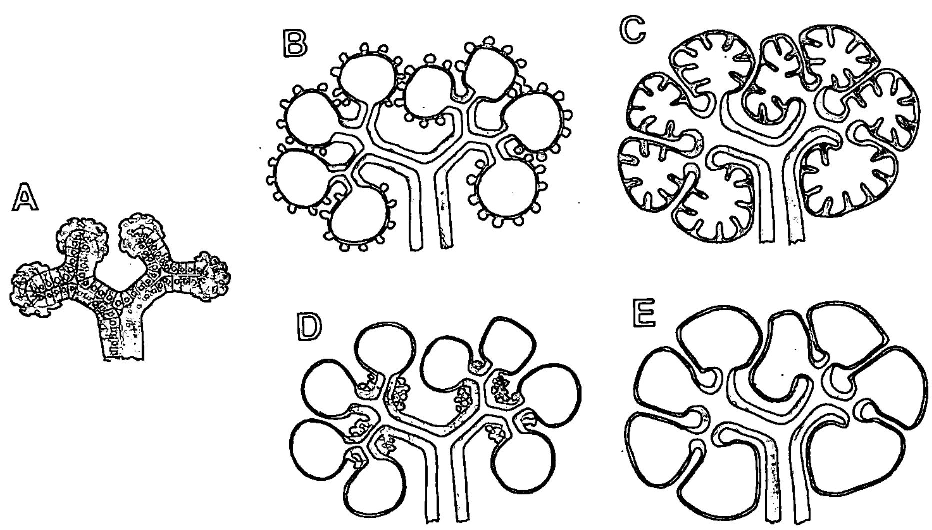

Fig. 7. Model of alveolar SMC development. Alveolar SMC progenitors (blue) originate at the pseudoglandular stage as clustered PDGFRα^+ mesenchymal cells located at the epithelial buds (A). In conjunction with the canalicular stage, these cells spread to acquire positions surrounding the prospective terminal sacs (B). During the terminal sac to alveolar stages, the cells down-regulate PDGFRα expression and up-regulate tropoelastin expression (black) (C). In PDGF-A$^{-/-}$ lungs the distal spreading of PDGFRα^+ progenitors does not occur (D), and consequently, alveolar septal elastin deposition (and alveogenesis) fails (E).

loss of septum formation in PDGF-A$^{-/-}$ mice. Irrespective of whether or not elastin deposition is a morphogenetic force in alveogenesis, the importance of elastin to alveolar septum integrity is supported by studies of the pathogenesis of human lung emphysema. In this condition(s) septal elastin destruction appears to be critical, brought about either by genetic anti-elastase deficiency, or by increased release of inflammatory elastases (Janoff, 1988; Muley et al., 1994; Snider, 1984). Thus although implying a common critical denominator, alveolar septal elastin, the pathogenesis of emphysema in human beings and in PDGF-A-deficient mice appears to be different.

Arteriolar reaction and cor pulmonale in PDGF-A$^{-/-}$ mice

Up-regulation of smooth muscle α-actin in blood vessel wall cells is often found in conjunction with hypertension, and is seen in hypertensive aorta (Clements et al., 1997), in arterioles in pulmonary hypertension (Jones et al., 1997) and in mesangial cells during the development of hypertensive renal damage (Kimura et al., 1996). Thus both the up-regulated expression of smooth muscle α-actin seen in the arterioles of the emphysematous lungs of 2-week-old PDGF-A$^{-/-}$ pups (this study), and the cor pulmonale seen at 3 weeks (Boström et al., 1996) are indicative of pulmonary hypertension. In human patients with emphysema, muscularization of pulmonary arterioles sometimes occurs, which leads to pulmonary hypertension and cor pulmonale (Marshall and Marshall, 1997). It is believed that the cause of these changes is persistent hypoxia, which leads to prolonged pulmonary vasoconstriction and secondary vascular changes (Marshall and Marshall, 1997; Riley et al., 1997). It can be assumed that the advanced and generalized emphysema of the PDGF-A$^{-/-}$ mice leads to hypoxia. Angiotensin II is known to up-regulate smooth muscle α-actin (Andrawis et al., 1996) and stimulate vascular smooth muscle cell hypertropy (Morrell et al., 1996; Patton et al., 1995), and is therefore a possible mediator of the vascular reaction seen in the emphysematous PDGF-A$^{-/-}$ lung.

In summary, the lung arteriolar phenotype and the cor pulmonale of PDGF-A$^{-/-}$ mice from 2 weeks of postnatal age may both be secondary to hypoxia occurring as a result of severe lung emphysema.

Generic features of PDGF-A and PDGF-B function

By phenotypical analysis of PDGF knockout mice, we have found generic features of PDGF-A and PDGF-B function. Three types of smooth muscle cells/myofibroblasts show an obligatory requirement for different PDGF isoforms during development; alveolar SMC depend on PDGF-A (Boström et al., 1996); this study) and microvascular pericytes and kidney glomerular mesangial cells depend on PDGF-B (Levéen et al., 1994; Lindahl et al., 1997; Soriano, 1994). In all three cases, locally produced PDGF appears to trigger PDGF receptor-positive progenitor cells to multiply and spread from a proximal to a distal location. A similar function may also be performed by PDGF-A during Xenopus gastrulation (Ataliotis et al., 1995), at which time mesodermal cells move along the blastocoel roof on a posterior-to-anterior route. Taken together, the available data thus suggest that PDGFs provide selective signals during embryonic development, by acting on the PDGF receptor-carrying progenitor cells and allowing for their proliferation and spreading on PDGF-producing endothelial or epithelial sheet/tubes. It is possible that this selective process involves proliferation and migration only, processes known to be regulated by PDGF in vitro (Betsholtz and Raines, 1997), but it may involve other functions as well, such as cell survival or differentiation.

We would like to thank Sara Beckman for technical assistance, and Drs J. Escobedo, J. Foster, W.D. Richardson, and P. Soriano for DNA probes. This study was supported by grants from the Swedish Cancer Foundation, the Swedish Medical Research Council, the Ingabritt and Arne Lundberg Research Foundation, the Cancer Research Campaign UK and the Wellcome Trust.

REFERENCES

Alescio, T., and Cassini, A. (1962). Induction in vitro of tracheal buds by pulmonary mesenchyme grafted on tracheal epithelium. *J. Exp. Zool.* **150**, 83-94.

Andrawis, N. S., Wang, E., and Abernethy, D. R. (1996). Endothelin-1 induces an increase in total protein synthesis and expression of the smooth muscle alpha-actin gene in vascular smooth muscle cells. *Life Sci.* **59**, 523-528.

Ataliotis, P., Symes, K., Chou, M. M., Ho, L., and Mercola, M. (1995). PDGF signalling is required for gastrulation in *Xenopus laevis*. *Development* **121**, 3099-3110.

Bellusci, S., Furuta, Y., Rush, M. G., Henderson, R., Winnier, G., and Hogan, B. L. M. (1997). Involvement of Sonic hedgehog (Shh) in mouse embryonic lung growth and morphogenesis. *Development* **124**, 53-63.

Bellusci, S., Henderson, R., Winnier, G., Oikawa, T., and Hogan, B. L. M. (1996). Evidence from normal expression and targeted misexpression that bone morphogenetic protein-4 (Bmp-4) plays a role in mouse embryonic lung morphogenesis. *Development* **122**, 1693-1702.

Betsholtz, C., and Raines, E. (1997). Platelet-derived growth factor: A key regulator of connective tissue cells in embryogenesis and pathogenesis. *Kidney Int.* **51**, 1361-1369.

Boström, H., Willetts, K., Pekny, M., Levéen, P., Lindahl, P., Hedstrand, H., Pekna, M., Hellström, M., Gebre-Medhin, S., Schalling, M., Nilsson, M., Kurland, S., Törnell, J., Heath, J. K., and Betsholtz, C. (1996). PDGF-A signaling is a critical event in lung alveolar myofibroblast development and alveogenesis. *Cell* **85**, 863-873.

Burri, P. H., and Weibel, E. R. (1977). Ultrastructure and morphometry of the developing lung. In *Development of the Lung, Part 1: Structural Development* (ed. W. A. Hodson), pp. 215-268. New York: Marcel Dekker.

Clements, M. L., Banes, A. J. and Faber, J. E. (1997). Effect of mechanical loading on vascular alpha 1D- and alpha 1B-adrenergic receptor expression. *Hypertension* **29**, 1156-1164.

Collett, A. J. and Des Biens, G. (1974). Fine structure of the myogenesis and elastogenesis in the developing rat lung. *Anat. Rec.* **179**, 343-360.

Emery, J. L. (1970). The postnatal development of the human lung and its implication for lung pathology. *Respiration* **27**, 41-50.

Fukuda, Y., Ferrans, V. J. and Crystal, R. G. (1983). The development of alveolar septa in fetal sheep lung. An ultrastructural and immunohistochemical study. *Am. J. Anat.* **167**, 405-439.

Goldin, G. V., Hindman, H. M. and Wessells, N. K. (1984). The role of cell proliferation and cellular shape change in branching morphogenesis of the embryonic mouse lung: analysis using aphidicolin and cytochalasins. *J. Exp. Zool.* **232**, 287-296.

Goldin, G. V. and Wessels, N. K. (1979). Mammalian lung development: the possible role of cell proliferation in the formation of supernumerary trachea buds and in branching morphogenesis. *J. Exp. Zool.* **208**, 337-346.

Heine, U. I., Munoz, E. F., Flanders, K. C., Roberts, A. B. and Sporn, M. B. (1990). Colocalization of TGF-beta 1 and collagen I and III and glycosaminoglycans during lung branching morphogenesis. *Development* **109**, 29-36.

Heldin, C.-H. (1992). Structural and functional studies of platelet-derived growth factor. *EMBO J.* **11**, 4251-4259.

Henrique, D., Adam, J., Myat, A., Chitnis, A., Lewis, J. and Ish-Horowicz, D. (1995). Expression of a Delta homologue in prospective neurons in the chick. *Nature* **375**, 787-790.

Hilfer, S. R. (1996). Morphogenesis of the lung: Control of embryonic and fetal branching. *Annu. Rev. Physiol.* **59**, 93-113.

Hilfer, S. R., Rayner, R. M. and Brown, J. W. (1985). Mesenchymal control of branching pattern in the fetal mouse lung. *Tissue Cell* **17**, 523-538.

Janoff, A. (1988). Emphysema: Proteinase-antiproteinase imbalance. In *Inflammation: Basic Principles and Clinical Correlates* (ed. J. Gallin et al.), pp. 803-825. New York: Raven Press.

Jones, P. L., Cowan, K. N. and Rabinovitch, M. (1997). Tenascin-C, proliferation and subendothelial fibronectin in progressive pulmonary vascular disease. *Am. J. Pathol.* **150**, 1349-1360.

Kaartinen, V., Voncken, J. W., Shuler, C., Warburton, D., Bu, D., Heisterkamp, N. and Groffen, J. (1995). Abnormal lung development and cleft palate in mice lacking TGF-beta3 indicates defects of epithelial-mesenchymal interaction. *Nature Genetics* **11**, 415-421.

Kapanchi, Y., Assimacopoulos, A., Irle, C., Zwahlen, A. and Gabbiani, G. (1974). Contractile interstitial cells in pulmonary alveolar septa: A possible regulator of ventilation/perfusion ratio? *J. Cell Biol.* **60**, 375-392.

Kapanchi, Y. and Gabbiani, G. (1997). Contractile cells in pulmonary alveolar tissue. In *The Lung. Scientific Foundations*, 2nd edition (ed. R. G. Crystal, J. B. West, E. R. Weibel and P. J. Barnes), pp. 697-707. Philadelphia: Lippincott-Raven Publishers.

Kimura, K., Suzuki, N., Ohba, S., Nagai, R., Hiroi, J., Mise, N., Tojo, A., Nagaoka, A., Hirata, Y., Goto, A., Yazaki, Y. and Omata, M. (1996). Hypertensive glomerular damage as revealed by the expression of alpha-smooth muscle actin and non-muscle myosin. *Kidney Int. Suppl.* **55**, S169-172.

Korfhagen, T. R., Swants, R. J., Wert, S. E., McCarty, J. M., Kerlakian, C. B., Glasser, S. W. and Whitsett, J. A. (1994). Respiratory epithelial cell expression of human transforming growth factor-alpha induces lung fibrosis in transgenic mice. *J. Clin. Invest.* **93**, 1691-1699.

Levéen, P., Pekny, M., Gebre-Medhin, S., Swolin, B., Larsson, E. and Betsholtz, C. (1994). Mice deficient for PDGF B show renal, cardiovascular and hematological abnormalities. *Genes Dev.* **8**, 1875-1887.

Lindahl, P., Johansson, B., Levéen, P. and Betsholtz, C. (1997). Pericyte loss and microaneurysm formation in PDGF-B-deficient mice. *Science* **277**, 242-245.

Marshall, B. E. and Marshall, C. (1997). Pulmonary hypertension. In *The Lung. Scientific Foundations*, 2nd edition (ed. R. G. Crystal, J. B. West, E. R. Weibel and P. J. Barnes), pp. 1581-1588. Philadelphia: Lippincott-Raven.

Miettinen, P. J., Berger, J. E., Meneses, J., Phung, Y., Pedersen, R. A., Werb, Z. and Derynck, R. (1995). Epithelial immaturity and multiorgan failure in mice lacking epidermal growth factor receptor. *Nature* **376**, 337-341.

Miller, W. S. (1921). The musculature of the finer divisions of the bronchial tree and its relation to certain pathological conditions. *Am. Rev. Tuberc.* **5**, 689-698.

Morrell, N. W., Grieshaber, S. S., Danilov, S. M., Majack, R. A. and Stenmark, K. R. (1996). Developmental regulation of angiotensin converting enzyme and angiotensin type1 receptor in the rat pulmonary circulation. *Am. J. Respir. Cell. Mol. Biol.* **14**, 526-537.

Muley, T., Wiebel, M., Schultz, V. and Ebert, W. (1994). Elastinolytic activity of alveolar macrophages in smoking-associated pulmonary emphysema. *Clin. Invest.* **72**, 269-276.

Noguchi, A., Reddy, R., Kursar, J. D., Parks, W. C. and Mecham, R. P. (1989). Smooth muscle isoactin and elastin in fetal bovine lung. *Exp. Lung Res.* **4**, 537-552.

Noguchi, A. and Samaha, H. (1991). Developmental changes in tropoelastin gene expression in the rat lung studied by in situ hybridization. *Am. J. Respir. Cell. Mol. Biol.* **5**, 571-578.

Orr-Urtreger, A. and Lonai, P. (1992). Platelet-derived growth factor-A and its receptor are expressed in separate but adjacent cell layers of the mouse embryo. *Development* **115**, 1045-1058.

Patton, W. F., Erdjument-Bromage, H., Marks, A. R., Pempst, P. and Taubman, M. B. (1995). Components of the protein synthesis and folding machinery are induced in vascular smooth muscle cells by hypertrophic and hyperplastic agents. Identification by comparative protein phenotyping and microsequencing. *J. Biol. Chem.* **270**, 21404-21410.

Peters, K., Werner, S., Liao, X., Wert, S. E., Whitsett, J. and Williams, L. T. (1994). Targeted expression of a dominant negative FGF receptor blocks branching morphogenesis and epithelial differentiation of the mouse lung. *EMBO J.* **13**, 3296-3301.

Ramachandran, R. K., Govindarajan, V., Seid, C. A., Patil, S. and Tomlinson, C. R. (1995). Role for platelet-derived growth factor-like and epidermal growth factor-like signaling pathways in gastrulation and spiculogenesis in the Lytechinus sea urchin embryo. *Dev. Dynam.* **204**, 77-88.

Riley, D., Thakker-Varia, S., Poiani, G. J. and Tozzi, C. A. (1997). Vascular remodelling. In *The Lung. Scientific Foundations*, 2nd edition (ed. R. G. Crystal, J. B. Weste, E. R. Weibel and P. J. Barnes), pp. 1589-1597. Philadelphia: Lippincott-Raven.

Schatteman, G. C., Loushin, C., Li, T. and Hart, C. E. (1996). PDGF-A is required for normal murine cardiovascular development. *Dev. Biol.* **176**, 133-142.

Serra, R., Pelton, R. W. and Moses, H. L. (1994). TGF-beta1 inhibits branching morphogenesis and N-myc expression in lung bud organ cultures. *Development* **120**, 2153-2161.

Simonet, W. S., Derose, M. L., Bucay, N., Nguyen, H. Q., Wert, S. E., Zhou, L., Ulich, T. R., Thomason, A., Danilenko, D. M. and Whitsett, J. A. (1995). Pulmonary malformations in transgenic mice expressing human keratinocyte growth factor in the lung. *Proc. Nat. Acad. Sci. USA* **92**, 12461-12465.

Snider, G. L. (1984). Two decades of research in the pathogenesis of emphysema. *Schweiz Med. Wochenschr.* **114**, 898-906.

Soriano, P. (1994). Abnormal kidney development and hematological disorders in PDGF beta-receptor mutant mice. *Genes Dev.* **8**, 1888-1896.

Soriano, P. (1997). The PDGF α receptor is required for neural crest cell development and for normal patterning of the somites. *Development* **124**, 2691-2700.

Ten Have-Opbroek, A. A. W. (1981). The development of the lung in mammals: an analysis of concepts and findings. *Am. J. Anat.* **162**, 201-219.

Ten Have-Opbroek, A. A. W. (1991). Lung development in the mouse embryo. *Exp. Lung Res.* **17**, 111-130.

Vaccaro, C. and Brody, J. S. (1978). Ultrastructure of developing alveoli. I. The role of the interstitial fibroblast. *Anat. Rec.* **192**, 457-480.

Wessels, N. K. (1970). Mammalian lung development: interactions in formation and morphogenesis of tracheal buds. *J. Exp- Zool.* **175**, 455-466.

Zhou, L., Dey, C. R., Wert, S. E. and Whitsett, J. A. (1996). Arrested lung morphogenesis in transgenic mice bearing an SP-C-TGF-beta1 chimeric gene. *Dev. Biol.* **175**, 227-238.

(Accepted 6 August 1997)